MATHGLM-VISION: SOLVING MATHEMATICAL PROBLEMS WITH MULTI-MODAL LARGE LANGUAGE MODEL

Anonymous authors
Paper under double-blind review

ABSTRACT

Large language models (LLMs) have demonstrated significant capabilities in mathematical reasoning, particularly with text-based mathematical problems. However, current multi-modal large language models (MLLMs), especially those specialized in mathematics, tend to focus predominantly on solving geometric problems but ignore the diversity of visual information available in other areas of mathematics. Moreover, the geometric information for these specialized mathematical MLLMs is derived from several public datasets, which are typically limited in diversity and complexity. To address these limitations, we aim to construct a fine-tuning dataset named MathVL, and develop a series of specialized mathematical MLLMs termed MathGLM-Vision by conducting Supervised Fine-Tuning (SFT) on MathVL with various parameter-scale backbones. To extensively evaluate the effectiveness of MathGLM-Vision, we conduct experiments on several public benchmarks and our curated MathVL-test benchmark consisting of 2,000 problems. Experimental results demonstrate that MathGLM-Vision achieves significant improvements compared with some existing models, including backbone models and open-source mathematical MLLMs. These findings indicate the importance of diversity dataset in enhancing the mathematical reasoning abilities of MLLMs. Both MathGLM-Vision model (based on CogVLM2, GLM-4V-9B) and MathVL-test will be open-sourced.

1 INTRODUCTION

Recent advancements in computational linguistics have led to substantial progress in solving mathematical problems using Large Language Models (LLMs) with multi-step reasoning processes (Lightman et al., 2023). For example, models like GPT-4 (Achiam et al., 2023), Qwen (Bai et al., 2023a), GLM-4 (Team et al., 2024), LLaMA (Touvron et al., 2023a;b) have demonstrated impressive performance on mathematical datasets such as GSM8K (Cobbe et al., 2021) and MATH (Hendrycks et al., 2021). Furthermore, the development of specialized mathematical models is expanding the potential of LLMs in this domain. These models, specifically designed for mathematical problem solving, include notable contributions such as WizardMath (Luo et al., 2023), MAmmoTH (Yue et al., 2023), MathCoder (Wang et al., 2023a), MetaMath (Yu et al., 2023), DeepSeekMath (Shao et al., 2024), and others (Yang et al., 2023; Yuan et al., 2023; Gou et al., 2023; Yue et al., 2024b; Mitra et al., 2024; Ying et al., 2024). These advancements highlight the growing proficiency of LLMs in handling intricate mathematical reasoning and problem-solving tasks.

Despite significant advancements, the majority of models designed for mathematical problem solving still rely predominately on textual representations. This limits their effectiveness in scenarios that require visual information. Notably, approximately 63% of mathematics questions in Chinese K12 education include visual elements, highlighting the critical role of visual information in comprehending and solving mathematical problems.

Therefore, a crucial question arises: **Is visual information essential for solving these mathematical problems that include visual elements?** To verify this, we conduct a series of insightful experiments comparing the performance of these models such as GPT-4o, Claude-3.5-Sonnet, Qwen-VL-Max, and Gemini-1.5-Pro on MathVL-test dataset, both with and without visual inputs. As shown in Figure 1, the results clearly demonstrate that the inclusion of visual elements significantly enhances the models' ability to accurately solve complex mathematical problems. Conversely, the exclusion of

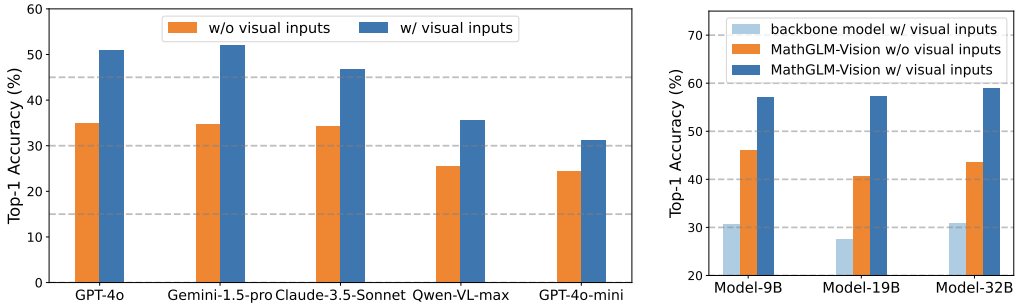

Figure 1: Insight experiments demonstrates the significance of visual information in solving mathematical problems. (Left) A performance comparison of different models with and without visual inputs on MathVL-test dataset. (Right) The accuracies of MathGLM-Vision on MathVL-test with and without visual inputs.

visual information leads to a pronounced decrease in performance, emphasizing the essential role that visual context plays in solving mathematical problems that incorporate visual elements.

Currently, multi-modal large language models (MLLMs) are at the forefront of efforts to integrate visual and textual information for solving mathematical problems. Close-source models such as GPT-4V (OpenAI, 2023), Gemini (Team et al., 2023), Claude3 (Anthropic, 2024), Qwen-VL (Bai et al., 2023b), along with several open-source MLLMs like CogVLM (Wang et al., 2023c; Hong et al., 2024), MiniGPT Zhu et al. (2023), LLaVA-1.5 Liu et al. (2024a), SPHINX-MoE Gao et al. (2024), and LLaVA-NeXT Liu et al., demonstrate substantial potential in addressing geometric reasoning challenges. Additionally, specialized geometric MLLMs like G-LLaVA Gao et al. (2023a), GeoGPT4V Cai et al. (2024) and Math-LLaVA Shi et al. (2024) are particularly focused on enhancing capabilities in this domain. However, these models still face several challenges and limitations that need to be addressed.

- *Current MLLMs, particularly those specialized in mathematics, predominantly focus on solving geometric problems and tend to overlook the diversity of visual information in mathematics. This visual information encompasses a broad spectrum of elements, including arithmetic, statistics, algebra and word problems, each integral to different mathematical domains beyond geometry.*
- *Current fine-tuning dataset for specialized mathematical MLLMs, typically sourced from public datasets like GeoQA and Geometry3K, often lack diversity and complexity. This limitation restricts the models' ability to effectively solve a broader range of mathematical problems.*
- *Current specialized mathematical MLLMs are predominantly designed to process single-image inputs and lack the capability to handle multiple images simultaneously. This limitation hampers their ability to tackle complex problems that necessitate the integration of information from multiple visual sources.*

In response to these challenges and limitations, we construct a fine-tuning dataset named **MathVL**, which encompasses both open-source data and our specially curated Chinese data collected from K12 education. The MathVL dataset is meticulously designed to incorporate a diverse range of mathematical problems, consisting of textual and visual inputs. For textual information, the MathVL dataset covers a variety of mathematical subjects such as arithmetic, algebra, geometry, statistics, and word problems. It includes various types of questions, including fill-in-the-blank, multiple-choice, and free-form. For visual information, the MathVL dataset involves elements like functions, statistical data, graphs, charts, LaTeX expressions, and geometric figures, providing a comprehensive resource for complex mathematical problem solving.

With our constructed MathVL dataset, we develop a series of specialized mathematical MLLMs, collectively referred to as **MathGLM-Vision**, with different parameter scales. Specifically, MathGLM-Vision-9B, MathGLM-Vision-19B and MathGLM-Vision-32B are fine-tuned on three backbone models: GLM-4V-9B, CogVLM2, and CogVLM-32B, respectively. Moreover, we establish a benchmark dataset named **MathVL-test,** which contains 2,000 problems designed to evaluate the ability of MathGLM-Vision and other MLLMs in solving mathematical problems involving multiple images. Through extensive evaluation experiments on three public benchmark datasets and one curated

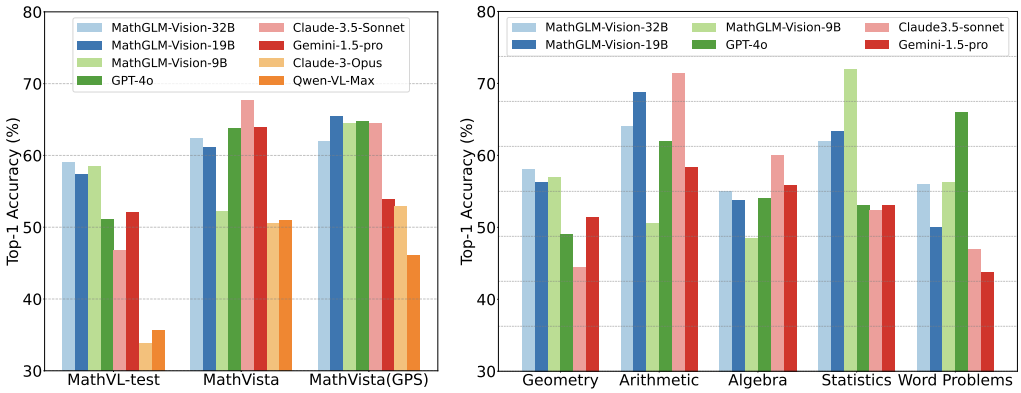

Figure 2: Performance comparison of the different multi-modal large language models. (Left) The accuracies of MathGLM-Vision and other MLLMs among three evaluation datasets. (Right) The accuracy of MathGLM-Vision and other MLLMs on MathVL-test across different categories.

MathVL-test, we validate the effectiveness of our MathGLM-Vision. The results in Figure 2 demonstrate that MathGLM-Vision exhibits superior performance in understanding and solving complex mathematical problems with visual elements compared to existing MLLMs. For instance, on the geometry problem solving (GPS) minitest split of MathVista (Lu et al., 2023), MathGLM-Vision-9B achieves a 39.68% relative improvement for GLM-4V-9B, MathGLM-Vision-19B achieves a 65.06% relative improvement for CogVLM2, and MathGLM-Vision-32B achieves a 51.05% relative improvement over CogVLM-32B. Last but not least, Both MathGLM-Vision model (based on CogVLM2, GLM-4V-9B) and MathVL-test will be open-sourced to facilitate the future development of this field.

We highlight our contributions as follows:

- **Data Perspective:** We construct MathVL, a diverse and comprehensive multi-modal mathematical supervised fine-tuning dataset that contains both textual and visual inputs.
- **Model Perspective:** We develop a suite of specialized mathematical multi-modal large language models, referred to as MathGLM-Vision, which demonstrates significant improvements on various mathematical benchmarks while maintaining general vision-language understanding capabilities.
- **Benchmark Perspective:** We establish a benchmark dataset called MathVL-test, which designed to evaluate the mathematical reasoning abilities of MLLMs using a multi-image format.

2 MathVL: Dataset Curation

To enhance the capabilities of MLLMs in solving mathematical problems, previous efforts (Chen et al., 2021; 2022; Cao & Xiao, 2022; Gao et al., 2023a) focus on constructing high-quality datasets. Nevertheless, the majority of these datasets fall into the category of Visual Question Answering (VQA), which generally involves descriptive or identification tasks rather than conventional mathematical problems. Furthermore, the answers in some public datasets like Geometry3K (Lu et al., 2021), GeoGPT4V (Cai et al., 2024), MathV360K (Shi et al., 2024) for standard mathematical questions are often too simplistic, usually providing only the final answer without the intermediate steps necessary for a thorough understanding. It is well-established that including step-by-step solutions can significantly enhance the reasoning capabilities of large language models (Wei et al., 2022; Lightman et al., 2023; Zhang et al., 2023; Wang et al., 2023b). Figure 3 demonstrates the distribution of answer lengths in current open-source mathematical datasets.

To address these issues, we construct a fine-tuning dataset MathVL, including both several public datasets and our curated Chinese dataset collected from K12 education levels. This dataset is meticulously crafted to encompass a diverse array of mathematical problems that incorporate visual information. Each problem is presented with detailed step-by-step solutions, aiming to enhance the problem-solving skills of MLLMs by providing them with both the context and the procedural knowledge necessary for effective reasoning and comprehension.

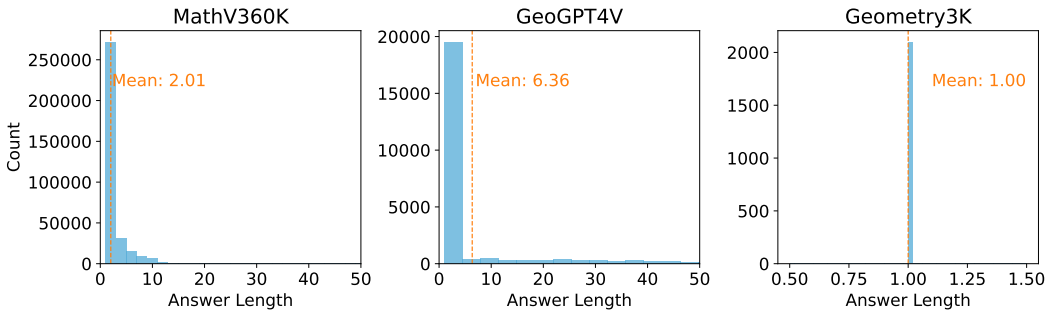

Figure 3: Analysis of answer lengths in several open-source mathematical datasets like MathV360K, GeoGPT4V, and Geometry3K.

Open-Source Data. We first collect open-source datasets from GeoQA+ (Cao & Xiao, 2022), Geometry3K (Lu et al., 2021), ChartQA (Masry et al., 2022), and UniGEO-Calculation (Chen et al., 2022). These datasets commonly serve as seed data for constructing enhanced datasets. Through observation and statistical analysis, we discover that 57% of the answers within these datasets are comprised of fewer than 50 words, indicating that many questions are answered directly without elaboration or explanation. To enrich these dataset with comprehensive step-by-step solutions, we employ GPT-4o to generate the detailed solutions for each question, thereby enhancing the learning and reasoning potential of these datasets. After generating the detailed answers, we perform a rigorous judgement process to ensure the accuracy of the solutions provided by GPT-4o. Additionally, we adopt a public instruction tuning dataset named Geo170K (Gao et al., 2023a), which is constructed using GeoQA+ and Geometry3K as seed data and contains more than 110K geometric question-answer pairs. We also incorporate another public dataset, GeomVerse (Kazemi et al., 2023), as part of our resources. In the end, the detailed statistics of the open-source datasets used in MathGLM-Vision is provided in Table 1.

Datasets	ChartQA	UniGeo-Calculation	Geometry3K	GeoQA+	Geo170K	GeomVerse	ALL
Samples	7,398	3,499	2,101	6,026	117,205	9,339	145,568

Table 1: The detailed statistics of the open-source datasets used in MathGLM-Vision.

Chinese Data Collected from K12 Education. We construct a dataset specifically focused on K12 education, comprising 341,346 mathematical problems with textual and visual inputs. This dataset is meticulously curated to encompass a board range of mathematical topics and difficulty levels tailored to the Chinese educational curriculum. It features various question types, such as multiple-choice, fill-in-the-blank, and free-form questions, spanning disciplines including arithmetic, algebra, geometry, statistics, and word problems. Mathematically, this dataset can be represented as $D^{\text{zh}}_{\text{MathVL}} = \{Q, A, I_s\}$, where Q represents the question, A represents the answer, and I_s represents one or more images associated with each question. To build this dataset, we first process the images by adding a white border around each image and enhancing their resolution to ensure that MLLMs can effectively recognize and interpret these images. This modification is crucial for facilitating the accurate extraction of visual information. Next, we extract 341,346 samples from a raw dataset containing 685,670 samples by implementing a selective filtering process. This selection is based on two specific criteria: (1) filtering out samples where the answer includes images or the question is incomplete, and (2) eliminating samples with answer that are fewer than 50 words in length to ensure the responses are sufficiently detailed for model training. After constructing this dataset, we categorize and analyze it based on mathematical topics associated with each question. Detailed statistics about the distribution of these categories are presented in Table 2. Figure 4 demonstrates some examples sampled from the constructed Chinese dataset, providing a visual representation of the mathematical topics of questions included. More dataset cases are provided in Appendix A.

Types	Arithmetic	Geometry	Algebra	Statistics	Word Problems	ALL
Samples	7,207	291,879	20,111	18,284	3,865	341,346

Table 2: Detailed statistics regarding the distribution used in MathGLM-Vision.

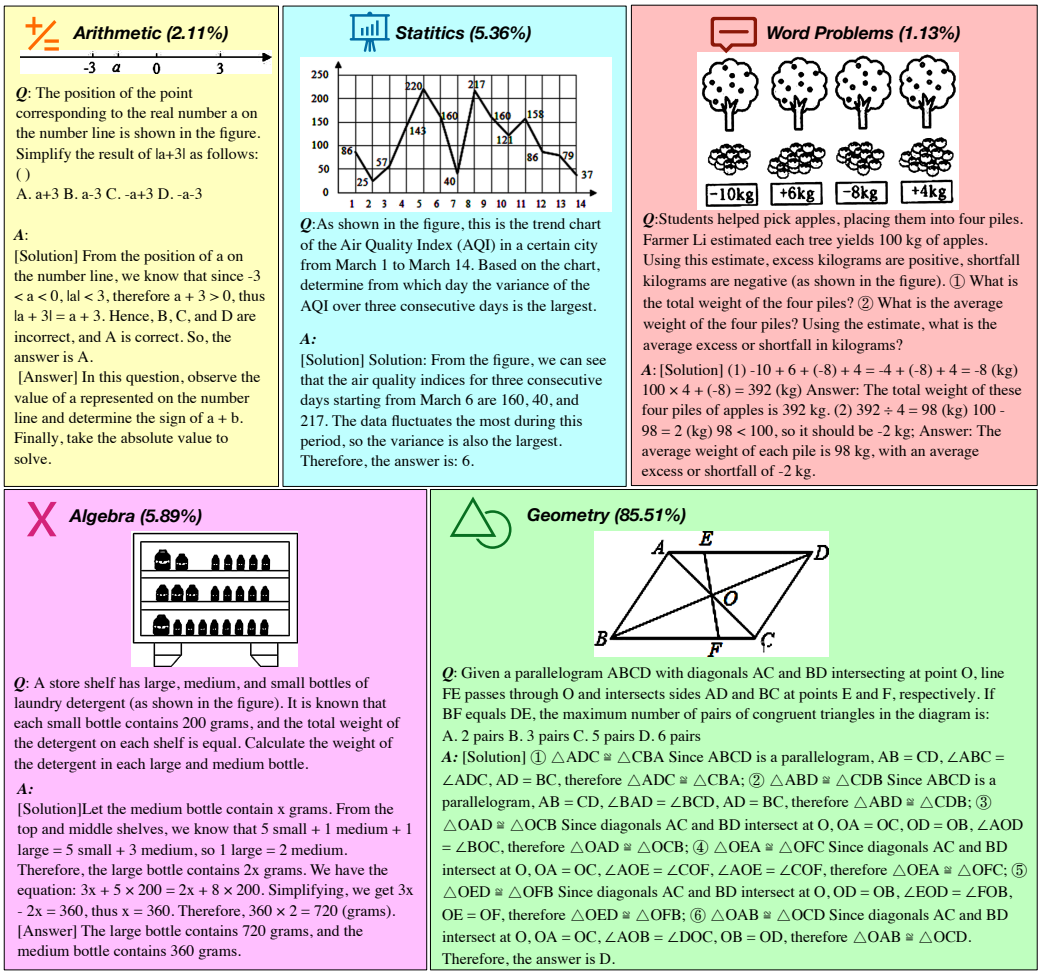

Figure 4: Examples sampled from the constructed Chinese dataset.

3 MATHGLM-VISION: MODEL TRAINING

Model Architecture. We employ CogVLM2 (Hong et al., 2024; Wang et al., 2023c) and GLM-4V-9B (GLM et al., 2024) architectures as our backbone models, and conduct Supervised Fine-Tuning (SFT) on our constructed MathVL dataset. Specifically, we utilize three pre-trained multi-modal large language models (MLLMs) for the fine-tuning process: GLM-4V-9B, CogVLM2-19B, and CogVLM-32B. This results in the development of three distinct variants of MathGLM-Vision, designated as MathGLM-Vision-9B, MathGLM-Vision-19B, and MathGLM-Vision-32B, respectively. Further details about the abovementioned three pre-trained MLLMs are available in Appendix B.

Model Training. To maintain the general vision-language understanding skills of MathGLM-Vision, we incorporate 19 open-source visual question-answering datasets (VQA datasets) into the MathVL dataset. More details about the task type and visual context of VQA datasets are provided in Appendix C. These datasets are meticulously selected to challenge and enhance the model's ability to interpret and integrate visual and textual information, ensuring it retains a broad understanding across various contexts. By merging these varied sources, we enhance MathGLM-Vision's specialized capabilities for mathematical problem-solving and simultaneously preserve its robustness in general vision-language tasks. In the end, we conduct supervised fine-tuning (SFT) across the combined VQA and MathVL datasets. The training process undergoes 35,000 iterations with a learning rate of 1e-5 and a batch size of 128. To ensure the stability of the training, we activate the visual encoder's parameters and adjust its learning rate to be one-tenth of that used for the remaining training parameters. The details of the SFT procedures are described in Appendix D.

4 EXPERIMENTS

4.1 EXPERIMENTAL SETUP

Evaluation Datasets. We assess our MathGLM-Vision using three well-established public benchmark datasets (MathVista (Lu et al., 2023), MathVerse (Zhang et al., 2024), and MATH-Vision (Wang et al., 2024) datasets) alongside our specially curated dataset MathVL-test benchmark. This benchmark comprises 2,000 sampled cases, distinct from those in the MathVL dataset, ensuring a rigorous and unbiased evaluation of MathGLM-Vision's capabilities. Additionally, we evaluate MathGLM-Vision's general vision-language understanding skills using the MMMU benchmark Yue et al. (2024a). Detailed descriptions for these benchmark datasets are provided in Appendix E.

Compared Models. We compare MathGLM-Vision with other Multi-Modal Large Language Models (MLLMs), including closed-source MLLMs such as Gemini (Team et al., 2023), GPT-4V (OpenAI, 2023), Claude3 (Anthropic, 2024), and Qwen-VL (Bai et al., 2023b), and open-source MLLMs like mPLUG-Owl (Ye et al., 2023), LLaMA-Adapter-V2 (Gao et al., 2023b), InstrctBLIP (Dai et al., 2024), LLaVA-1.5 (Liu et al.), ShareGPT4V (Chen et al., 2023), SPHINX (Gao et al., 2024), InternLM-XC2 (Dong et al., 2024), and InternVL (Chen et al., 2024). Additionally, we compare MathGLM-Vision with recent specialized mathematical MLLMs, including G-LLaVA (Gao et al., 2023a), LLaVA-1.5-G (Cai et al., 2024), ShareGPT4V-G (Cai et al., 2024), and Math-LLaVA (Shi et al., 2024).

Evaluation Metrics. We adopt top-1 accuracy to evaluate our MathGLM-Vision across MathVista-GPS, MathVista, MathVerse, MATH-V, and MathVL-test benchmarks. Our evaluation process follows the pipeline outlined in the aforementioned benchmark datasets, which involves using LLMs to extract predicted answers from the model's responses. Accuracy is then calculated by comparing these extracted answers against the ground truths.

4.2 MAIN RESULTS

Results on public benchmark datasets. To comprehensively assess the ability of MathGLM-Vision in solving mathematical problems, we evaluate its performance against other MLLMs across several public benchmark datasets. Table 3 demonstrates the overall results from these evaluations. The experimental results indicate that our constructed MathVL dataset can significantly improve MathGLM-Vision's mathematical reasoning capabilities. For example, MathGLM-Vision-9B achieves a 64.42% accuracy on the MathVista-GPS dataset, marking a substantial 39.68% improvement over its backbone model, GLM-4V-9B. Besides, across various parameter scales, MathGLM-Vision consistently surpass all backbone models on different evaluation benchmarks, highlighting the significant enhancements that MathVL brings to the MathGLM-Vision's problem-solving skills. Notably, MathGLM-Vision outperforms all open-source specialized mathematical MLLMs across various benchmarks. The superior performance suggests that the high-quality and diverse data, complete with detailed step-by-step solutions, are crucial for improving MLLM's mathematical reasoning capabilities. More importantly, MathGLM-Vision-32B outperforms even the advanced GPT-4V on the more challenging MATH-V benchmark, demonstrating its superior capacity to tackle complex mathematical problems. Detailed experimental results on public benchmark datasets across different task types can be found in Appendix F.

Results on MathVL-test. We also evaluate MathGLM-Vision and several close-source MLLMs using our specially constructed MathVL-test benchmark. As depicted in Table 4, the results clearly demonstrate that MathGLM-Vision significantly outperforms both its backbone models and other leading closed-source MLLMs across various model sizes. Specifically, our MathGLM-Vision-32B outperforms the advanced GPT-4o with a significant margin, achieving an accuracy of 59.00% compared to GPT-4o's 51.05%. Compared to the backbone model, GLM-4V-9B, MathGLM-Vision-9B achieves an impressive accuracy of 57.05% with a significant improvement of 86.5%. This superior performance suggests that MathGLM-Vision, when conducting SFT on the MathVL dataset, notably enhances its capability to tackle complex Chinese mathematical problems. Additionally, we report the accuracy across various categories, as illustrated in Figure 2 (See Right). MathGLM-Vision significantly outperforms other advanced MLLMs in the domains of geometry and statistics. In

Model	Input	LLM	MathVista (GPS)	MathVista	MathVerse	MATH-V
Closed Source Models						
Gemini Pro	*Q, I*	-	40.40	45.20	36.80	17.66
Gemini-1.5-Pro	*Q, I*	-	53.85	63.90	51.08	19.24
GPT-4V	*Q, I*	-	50.50	49.90	50.80	22.76
GPT-4-turbo	*Q, I*	-	58.25	58.10	43.50	30.26
GPT-4o	*Q, I*	-	64.71	63.80	56.65	30.39
Claude3-Opus	*Q, I*	-	52.91	50.50	31.77	27.13
Claude3.5-Sonnet	*Q, I*	-	64.42	67.70	48.98	37.99
Qwen-VL-Plus	*Q, I*	-	33.01	43.30	19.10	10.72
Qwen-VL-Max	*Q, I*	-	46.12	51.00	35.90	15.59
Open Source Models						
General Multi-modal LLMs						
mPLUG-Owl	*Q, I*	LLaMA-7B	23.60	22.20	12.47	9.84
LLaMA-Adapter-V2	*Q, I*	LLaMA-7B	25.50	23.90	4.50	9.44
InstructBLIP	*Q, I*	Vicuna-7B	20.70	25.30	15.36	10.12
LLaVA-1.5	*Q, I*	Vicuna-13B	24.04	27.60	12.70	11.12
ShareGPT4V	*Q, I*	Vicuna-13B	38.35	29.30	16.20	11.88
SPHINX-MoE	*Q, I*	Mixtral 8*7B	31.20	42.30	19.60	14.18
SPHINX-Plus	*Q, I*	LLaMA2-13B	16.40	36.70	14.70	9.70
InternLM-XC2	*Q, I*	InternLM2-7B	63.00	57.60	24.40	14.54
InternVL-1.2-Plus	*Q, I*	Nous-Hermes-2-Yi-34B	61.10	59.90	21.70	16.97
Geo-Multi-modal LLMs						
G-LLaVA	*Q, I*	LLaMA2-7B	53.40	28.46	12.70	12.07
G-LLaVA	*Q, I*	LLaMA2-13B	56.70	35.84	14.59	13.27
LLaVA-1.5-G	*Q, I*	Vicuna-7B	32.69	45.22	13.96	14.13
LLaVA-1.5-G	*Q, I*	Vicuna-13B	36.54	48.34	15.61	14.88
ShareGPT4V-G	*Q, I*	Vicuna-7B	32.69	45.07	16.24	12.86
ShareGPT4V-G	*Q, I*	Vicuna-13B	43.27	49.14	16.37	14.45
Math-LLaVA	*Q, I*	Vicuna-13B	57.70	46.60	19.04	15.69
MathGLM-Vision and Backbone Models						
GLM-4V-9B	*Q, I*	GLM-4-9B	46.12	46.70	35.66	15.31
MathGLM-Vision-9B	*Q, I*	GLM-4-9B	**64.42**	**52.20**	**44.20**	**19.18**
CogVLM2	*Q, I*	LLaMA-3-8B	39.61	40.85	25.76	13.20
MathGLM-Vision-19B	*Q, I*	LLaMA-3-8B	**65.38**	**61.10**	**42.50**	**21.64**
CogVLM-32B	*Q, I*	GLM2-32B	41.06	40.04	35.28	19.32
MathGLM-Vision-32B	*Q, I*	GLM2-32B	**62.02**	**62.40**	**49.20**	**26.51**

Table 3: **Results on several public benchmark datasets.** Comparison of model performance on the testmini set of MathVista and geometry problem solving (GPS) of MathVista. For MathVerse dataset, results are evaluated on Vision Dominant with CoT-E. For MATH-V dataset, all 3,040 samples included in the data are evaluated.

contrast, Claude3.5-Sonnet excels in algebra and arithmetic, demonstrating superior performance. Meanwhile, MathGLM-Vision-19B ranks second in performance in the domain of arithmetic, showing its strong abilities in this area as well. GPT-4o exhibits the highest performance in word problems domain, while MathGLM-Vision also exhibits robust performance, surpassing both Gemini-1.5-Pro and Claude3.5-Sonnet in this category.

4.3 GENERALIZABILITY OF MATHGLM-VISION

In addition to its proficiency in mathematical reasoning, we further assess MathGLM-Vision's capabilities in general vision-language understanding by conducting experiments on the MMMU benchmark. This benchmark is specifically designed to evaluate the ability of models to comprehend and process information across a variety of academic and professional disciplines, providing a comprehensive test of general vision-language understanding. Table 5 shows the performance of MathGLM-Vision, a specific variant fine-tuned exclusively on MathVL without the inclusion of VQA datasets, and backbone models. Compared to CogVLM2, MathGLM-Vision-19B achieves comparable performance in terms of generalizability, underscoring its capacity for simultaneous

Model	Input	LLM Size	MathVL-test
Gemini-1.5-Pro	*Q*, *I*	-	52.03
GPT-4V	*Q*, *I*	-	35.89
GPT-4-turbo	*Q*, *I*	-	42.19
GPT-4o	*Q*, *I*	-	51.05
Claude3.5-Sonet	*Q*, *I*	-	46.84
Claude3-Opus	*Q*, *I*	-	33.77
Qwen-VL-Plus	*Q*, *I*	-	28.50
Qwen-VL-Max	*Q*, *I*	-	35.61
GLM-4V-9B	*Q*, *I*	9B	30.59
MathGLM-Vision-9B	*Q*, *I*	9B	**57.05**
CogVLM2	*Q*, *I*	8B	27.47
MathGLM-Vision-19B	*Q*, *I*	8B	**57.30**
CogVLM-32B	*Q*, *I*	32B	30.86
MathGLM-Vision-32B	*Q*, *I*	32B	**59.00**

Table 4: **Results on MathVL-test.** A detailed comparison of the performance of MathGLM-Vision and various other leading close-source MLLMs on the MathVL-test benchmark.

multi-modal understanding and mathematical reasoning. However, MathGLM-Vision-32B shows a slight reduction in performance across multiple categories on the MMMU benchmark. Besides, MathGLM-Vision, when fine-tuned with VQA datasets, outperforms its variant lacking VQA datasets. This indicates that omitting VQA datasets from the fine-tuning process limits the general vision-language understanding abilities. Thus, the SFT process using our MathVL incorporated with VQA datasets not only enhances MathGLM-Vision's mathematical reasoning abilities but also preserves its generalizability.

Model	MMMU	Art & Design	Business	Sci.	Health & Med.	Human. & Social Sci.	Tech. & Eng.
CogVLM2	40.2	58.3	30.0	26.7	**41.3**	38.6	**53.3**
w/o VQA datasets	38.1	60.8	28.7	**34.0**	36.7	43.3	32.9
MathGLM-Vision-19B	**40.2**	**63.3**	**37.3**	27.3	36.0	**46.7**	37.6
CogVLM-32B	**42.9**	**63.3**	**31.3**	32.0	**43.3**	**62.5**	**36.7**
w/o VQA datasets	38.6	62.5	26.7	28.0	34.0	56.7	33.8
MathGLM-Vision-32B	40.0	60.0	28.7	**34.0**	38.7	52.5	34.8

Table 5: Generalizability of MathGLM-Vision on the MMMU benchmark.

4.4 Further Analysis

Effect of Chinese Dataset. To validate the effectiveness of the adopted Chinese dataset in MathVL, we conduct an extended experiment that involves fine-tuning GLM-4V-9B with open-source datasets, deliberately excluding Chinese data collected from K12 education. Table 6 shows a comparison of performance results. Compared to the backbone model GLM-4V-9B, a variant MathGLM-Vision-9B that undergoes SFT exclusively with open-source data exhibits significant improvement on the minitest of MathVista, particularly in geometry problem solving (GPS) and geometry reasoning (GEO). This indicates that fine-tuning on diverse open-source data can markedly enhance model performance in specific mathematical areas. MathGLM-Vision, incorporating both open-source data and Chinese data, outperforms the variant tuned only with open-source data on the minitest of MathVista, highlighting the significant value added by integrating the Chinese dataset in the training process. Notably, compared to the variant without Chinese data, MathGLM-Vision achieves a significantly higher accuracy on the MathVL-test benchmark. These findings confirm that the inclusion of the Chinese dataset not only enhances the model's capability in handling complex mathematical problems but also contributes significantly to its overall performance on a diverse set of tasks within MathVista.

Effect of VQA Datasets. To explore the effect of VQA datasets on the performance of MathGLM-Vision, an extended experiment can be designed where SFT is applied exclusively to mathematical

Model	MathVista GPS	GEO	ALL	MathVL-test
GLM-4V-9B	46.12	44.35	46.70	30.59
+ SFT on Open-source Data	62.98	61.51	50.40	47.55
MathGLM-Vision-9B	64.42	62.34	52.20	57.25

Table 6: Effect of the constructed Chinese data.

Model	MathVista GPS	GEO	ALL
GLM-4V-9B	46.12	44.35	46.70
MathGLM-Vision-9B	64.42	62.34	52.20
- SFT on VQA Datasets	61.54	58.58	41.34

Table 7: Effect of the VQA datasets.

datasets, deliberately excluding VQA datasets. Table 7 demonstrates the performance comparison achieved by different models on MathVista. Compared to the backbone model GLM-4V-9B, a variant of MathGLM-Vision-9B achieves significant improvements on geometry problem solving (GPS) and geometry Reasoning (GEO). However, it exhibits a decline in the overall accuracy on the minitest of MathVista (ALL). The decline can be attributed to the composition of MathVista, which comprises five tasks, with question-answering types (such as graphical question-answering, textbook question-answering, and visual question-answering) comprising up to 60.6% of the tasks. Omitting VQA training in MathGLM-Vision impacts the model's ability to effectively process and respond to these multi-modal questions. Notably, within specific subsets of MathVista, such as GPS and GEO, a variant of MathGLM-Vision-9B slightly below the standard MathGLM-Vision-9B. This observation suggests that VQA datasets are crucial for preserving overall multi-modal understanding, their impact may vary depending on different task types. Besides, VQA datasets can indirectly bolster mathematical reasoning skills, which in turn enhances image recognition capabilities.

4.5 Error Analysis

We meticulously analyze the causes of errors in MathGLM-Vision-32B on the MathVL-test benchmark and illustrate the distribution of these errors in Figure 5. We summarize these errors in MathGLM-Vision-32B into five types: reasoning error, knowledge error, vision recognition error, calculation error, and question misunderstood error. The most prevalent type of errors, accounting for 69.1% of the total, is identified as Reasoning Error. This indicates a significant challenge in the MathGLM-Vision-32B's logical deductions and inferential reasoning. Improving these capabilities can dramatically enhance the MathGLM-Vision-32B's overall performance. Knowledge Error, which made up 12.7% of the errors, relates to the model's misapplicaion or lack of specific factual information. Vision Recognition Error accounts for 11.4% of the total errors and involves inaccuracies in interpreting visual data. This type of error can be reduced through the implementation of more advanced vision encoders. Furthermore, the fact that Calculation Error constitutes only 4.3% of the errors suggests that MathGLM-Vision-32B demonstrates considerable robustness in numerical and computational tasks. Lastly, Question Misunderstood Error, which constitutes 2.5% of the total, occurs when the model fails to correctly interpret question. Enhancing natural language processing capabilities and refining context understanding can significantly reduce these types of errors. Addressing these identified error types through targeted enhancements can significantly boost the overall effectiveness of MathGLM-Vision-32B. Figure 6 demonstrate some cases of the Calculation Error category. More detailed examples of these errors can be found in Appendix G.

5 Related Works

Multi-Modal Language Model. The development of Multi-Modal Language Models (MLLMs) have emerged as a significant area of research, which are designed to integrate information from multiple modalities—typically text and images—to perform tasks that require a holistic understanding of both visual and linguistic inputs. Pioneering efforts such as ViLBERT Lu et al. (2019) and LXMERT Tan & Bansal (2019) have advanced this field by conducting the joint pre-training on image-text datasets. They process text and image inputs separately before fusing them for final task layers, significantly improving performance on tasks like image captioning and visual question answering. The continues evolution of MLLMs has lead to innovations in data fusion techniques. Notable models such as CLIP Radford et al. (2021), ALIGN Jia et al. (2021), and BLIP Li et al. (2022) have adopted contrastive learning paradigms to align visual and language information from billions of image-text pairs. Concurrently, the success of LLMs Brown et al. (2020); Du et al. (2021); Zeng et al. (2022); Le Scao et al. (2023); Bai et al. (2022); Touvron et al. (2023a); Ouyang et al. (2022);

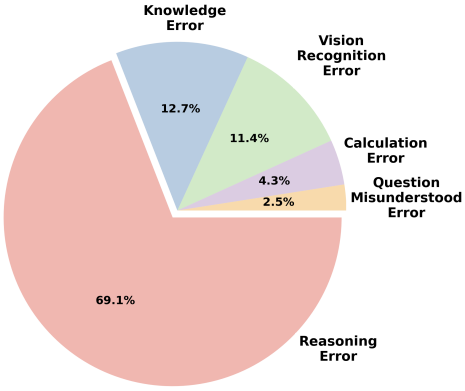

Figure 5: Error distribution of MathGLM-Vision-32B.

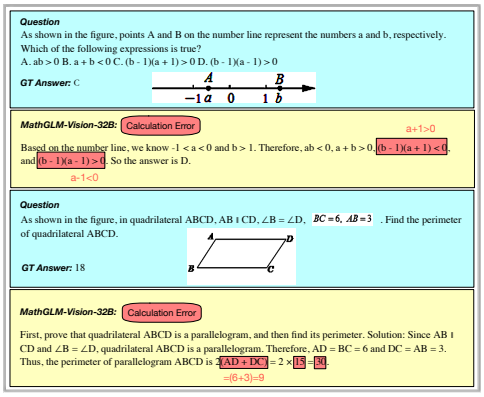

Figure 6: Cases of Calculation Error category.

Hoffmann et al. (2022); Smith et al. (2022); Chowdhery et al. (2023) facilitates the integration of LLMs into multi-modal tasks by utilizing pre-training alignment and visual instruction tuning, leading to the emergence of multi-modal language models (MLLMs) Liu et al. (2024b); Liu et al.; Wang et al. (2023c); Li et al. (2023); Dai et al. (2024); Bai et al. (2023a). Despite MLLMs have demonstrated remarkable capabilities on tasks such as image caption and visual question answering, they stall face significant challenges in solving mathematical problems that involve visual information Yue et al. (2024a); Lu et al. (2023); Zhang et al. (2024); Wang et al. (2024).

Mathematical Reasoning. Recently, math-specific LLMs Azerbayev et al. (2023); Wang et al. (2023a); Yue et al. (2024b); Ying et al. (2024); Yu et al. (2023); Yue et al. (2023); Yuan et al. (2023); Luo et al. (2023) have demonstrated remarkable abilities in handling mathematical reasoning tasks that only involve textual information. These models have been specifically trained on web-scale instruction mathematical dataset or fine-tuned on specialized mathematical problem sets. For instance, WizardMath Luo et al. (2023) and MetaMath Yu et al. (2023) have implemented data augmentation methods to enhance the models' ability to understand and solve mathematical problems by enriching the MATH Hendrycks et al. (2021) and GSM8K Cobbe et al. (2021) datasets. Recent research has also focused on creating specialized MLLMs for mathematical tasks. UniGeo Chen et al. (2022) and UniMath Liang et al. (2023) have demonstrated enhanced datasets and conventional deep learning approaches for geometric problem solving. MLLMs like G-LLaVA Gao et al. (2023a), GeoGPT4V Cai et al. (2024), and Math-LLaVA Shi et al. (2024) are tailored for mathematical problem solving, incorporating both geometric understanding and algebraic reasoning. Additionally, several benchmark datasets Yue et al. (2024a); Lu et al. (2023); Zhang et al. (2024); Wang et al. (2024) are proposed to evaluate the multi-modal mathematical reasoning abilities of MLLMs.

6 Conclusion

In this paper, we attempt to address the issues in current mathematical MLLMs. We construct a fine-tuning dataset named MathVL, upon which we conduct a Supervised Fine-Tuning (SFT) process. This initiative results in the development of a series of enhanced MLLMs, designated as MathGLM-Vision. Specially, MathGLM-Vision contains three variations: MathGLM-Vision-9B, MathGLM-Vision-19B, and MathGLM-Vision-32B, each fine-tuned on different backbone models: GLM-4-V, CogVLM2, and CogVLM-32B, respectively. These developed MathGLM-Vision significantly improve the capabilities of mathematical reasoning, achieving substantial performance improvements. Relative to their respective backbone models, MathGLM-Vision-9B, MathGLM-Vision-19B, and MathGLM-Vision-32B show improvements of 39%, 65%, and 53.7% on the Geometry Problem Solving (GPS) minitest split of MathVista, demonstrating the effectiveness of MathVL in enhancing the mathematical problem-solving abilities of MLLMs. Additionally, we evaluate the effectiveness of MathGLM-Vision on our curated MathVL-test benchmark. Experimental results reveal that MathGLM-Vision not only surpass their backbone models in specialized mathematical tests but also preserve the generalizability capabilities in general vision-language understanding domains.

REFERENCES

Josh Achiam, Steven Adler, Sandhini Agarwal, Lama Ahmad, Ilge Akkaya, Florencia Leoni Aleman, Diogo Almeida, Janko Altenschmidt, Sam Altman, Shyamal Anadkat, et al. Gpt-4 technical report. *arXiv preprint arXiv:2303.08774*, 2023.

Anthropic. The claude 3 model family: Opus, sonnet, haiku. 2024. URL https://www-cdn.anthropic.com/de8ba9b01c9ab7cbabf5c33b80b7bbc618857627/Model_Card_Claude_3.pdf.

Zhangir Azerbayev, Hailey Schoelkopf, Keiran Paster, Marco Dos Santos, Stephen McAleer, Albert Q Jiang, Jia Deng, Stella Biderman, and Sean Welleck. Llemma: An open language model for mathematics. *arXiv preprint arXiv:2310.10631*, 2023.

Jinze Bai, Shuai Bai, Yunfei Chu, Zeyu Cui, Kai Dang, Xiaodong Deng, Yang Fan, Wenbin Ge, Yu Han, Fei Huang, et al. Qwen technical report. *arXiv preprint arXiv:2309.16609*, 2023a.

Jinze Bai, Shuai Bai, Shusheng Yang, Shijie Wang, Sinan Tan, Peng Wang, Junyang Lin, Chang Zhou, and Jingren Zhou. Qwen-vl: A frontier large vision-language model with versatile abilities. *arXiv preprint arXiv:2308.12966*, 2023b.

Yuntao Bai, Andy Jones, Kamal Ndousse, Amanda Askell, Anna Chen, Nova DasSarma, Dawn Drain, Stanislav Fort, Deep Ganguli, Tom Henighan, et al. Training a helpful and harmless assistant with reinforcement learning from human feedback. *arXiv preprint arXiv:2204.05862*, 2022.

Tom Brown, Benjamin Mann, Nick Ryder, Melanie Subbiah, Jared D Kaplan, Prafulla Dhariwal, Arvind Neelakantan, Pranav Shyam, Girish Sastry, Amanda Askell, et al. Language models are few-shot learners. *Advances in neural information processing systems*, 33:1877–1901, 2020.

Shihao Cai, Keqin Bao, Hangyu Guo, Jizhi Zhang, Jun Song, and Bo Zheng. Geogpt4v: Towards geometric multi-modal large language models with geometric image generation. *arXiv preprint arXiv:2406.11503*, 2024.

Jie Cao and Jing Xiao. An augmented benchmark dataset for geometric question answering through dual parallel text encoding. In *Proceedings of the 29th International Conference on Computational Linguistics*, pp. 1511–1520, 2022.

Jiaqi Chen, Jianheng Tang, Jinghui Qin, Xiaodan Liang, Lingbo Liu, Eric P Xing, and Liang Lin. Geoqa: A geometric question answering benchmark towards multimodal numerical reasoning. *arXiv preprint arXiv:2105.14517*, 2021.

Jiaqi Chen, Tong Li, Jinghui Qin, Pan Lu, Liang Lin, Chongyu Chen, and Xiaodan Liang. Unigeo: Unifying geometry logical reasoning via reformulating mathematical expression. *arXiv preprint arXiv:2212.02746*, 2022.

Lin Chen, Jisong Li, Xiaoyi Dong, Pan Zhang, Conghui He, Jiaqi Wang, Feng Zhao, and Dahua Lin. Sharegpt4v: Improving large multi-modal models with better captions. *arXiv preprint arXiv:2311.12793*, 2023.

Zhe Chen, Jiannan Wu, Wenhai Wang, Weijie Su, Guo Chen, Sen Xing, Muyan Zhong, Qinglong Zhang, Xizhou Zhu, Lewei Lu, et al. Internvl: Scaling up vision foundation models and aligning for generic visual-linguistic tasks. In *Proceedings of the IEEE/CVF Conference on Computer Vision and Pattern Recognition*, pp. 24185–24198, 2024.

Aakanksha Chowdhery, Sharan Narang, Jacob Devlin, Maarten Bosma, Gaurav Mishra, Adam Roberts, Paul Barham, Hyung Won Chung, Charles Sutton, Sebastian Gehrmann, et al. Palm: Scaling language modeling with pathways. *Journal of Machine Learning Research*, 24(240):1–113, 2023.

Karl Cobbe, Vineet Kosaraju, Mohammad Bavarian, Mark Chen, Heewoo Jun, Lukasz Kaiser, Matthias Plappert, Jerry Tworek, Jacob Hilton, Reiichiro Nakano, et al. Training verifiers to solve math word problems. *arXiv preprint arXiv:2110.14168*, 2021.

Wenliang Dai, Junnan Li, Dongxu Li, Anthony Meng Huat Tiong, Junqi Zhao, Weisheng Wang, Boyang Li, Pascale N Fung, and Steven Hoi. Instructblip: Towards general-purpose vision-language models with instruction tuning. *Advances in Neural Information Processing Systems*, 36, 2024.

Xiaoyi Dong, Pan Zhang, Yuhang Zang, Yuhang Cao, Bin Wang, Linke Ouyang, Xilin Wei, Songyang Zhang, Haodong Duan, Maosong Cao, et al. Internlm-xcomposer2: Mastering free-form text-image composition and comprehension in vision-language large model. *arXiv preprint arXiv:2401.16420*, 2024.

Zhengxiao Du, Yujie Qian, Xiao Liu, Ming Ding, Jiezhong Qiu, Zhilin Yang, and Jie Tang. Glm: General language model pretraining with autoregressive blank infilling. *arXiv preprint arXiv:2103.10360*, 2021.

Jiahui Gao, Renjie Pi, Jipeng Zhang, Jiacheng Ye, Wanjun Zhong, Yufei Wang, Lanqing Hong, Jianhua Han, Hang Xu, Zhenguo Li, et al. G-llava: Solving geometric problem with multi-modal large language model. *arXiv preprint arXiv:2312.11370*, 2023a.

Peng Gao, Jiaming Han, Renrui Zhang, Ziyi Lin, Shijie Geng, Aojun Zhou, Wei Zhang, Pan Lu, Conghui He, Xiangyu Yue, et al. Llama-adapter v2: Parameter-efficient visual instruction model. *arXiv preprint arXiv:2304.15010*, 2023b.

Peng Gao, Renrui Zhang, Chris Liu, Longtian Qiu, Siyuan Huang, Weifeng Lin, Shitian Zhao, Shijie Geng, Ziyi Lin, Peng Jin, et al. Sphinx-x: Scaling data and parameters for a family of multi-modal large language models. *arXiv preprint arXiv:2402.05935*, 2024.

Team GLM, Aohan Zeng, Bin Xu, Bowen Wang, Chenhui Zhang, Da Yin, Diego Rojas, Guanyu Feng, Hanlin Zhao, Hanyu Lai, et al. Chatglm: A family of large language models from glm-130b to glm-4 all tools. *arXiv preprint arXiv:2406.12793*, 2024.

Zhibin Gou, Zhihong Shao, Yeyun Gong, Yujiu Yang, Minlie Huang, Nan Duan, Weizhu Chen, et al. Tora: A tool-integrated reasoning agent for mathematical problem solving. *arXiv preprint arXiv:2309.17452*, 2023.

Dan Hendrycks, Collin Burns, Saurav Kadavath, Akul Arora, Steven Basart, Eric Tang, Dawn Song, and Jacob Steinhardt. Measuring mathematical problem solving with the math dataset. *arXiv preprint arXiv:2103.03874*, 2021.

Jordan Hoffmann, Sebastian Borgeaud, Arthur Mensch, Elena Buchatskaya, Trevor Cai, Eliza Rutherford, Diego de Las Casas, Lisa Anne Hendricks, Johannes Welbl, Aidan Clark, et al. Training compute-optimal large language models. *arXiv preprint arXiv:2203.15556*, 2022.

Wenyi Hong, Weihan Wang, Ming Ding, Wenmeng Yu, Qingsong Lv, Yan Wang, Yean Cheng, Shiyu Huang, Junhui Ji, Zhao Xue, et al. Cogvlm2: Visual language models for image and video understanding. *arXiv preprint arXiv:2408.16500*, 2024.

Chao Jia, Yinfei Yang, Ye Xia, Yi-Ting Chen, Zarana Parekh, Hieu Pham, Quoc Le, Yun-Hsuan Sung, Zhen Li, and Tom Duerig. Scaling up visual and vision-language representation learning with noisy text supervision. In *International conference on machine learning*, pp. 4904–4916. PMLR, 2021.

Mehran Kazemi, Hamidreza Alvari, Ankit Anand, Jialin Wu, Xi Chen, and Radu Soricut. Geomverse: A systematic evaluation of large models for geometric reasoning. *arXiv preprint arXiv:2312.12241*, 2023.

Teven Le Scao, Angela Fan, Christopher Akiki, Ellie Pavlick, Suzana Ilić, Daniel Hesslow, Roman Castagné, Alexandra Sasha Luccioni, François Yvon, Matthias Gallé, et al. Bloom: A 176b-parameter open-access multilingual language model. 2023.

Junnan Li, Dongxu Li, Caiming Xiong, and Steven Hoi. Blip: Bootstrapping language-image pre-training for unified vision-language understanding and generation. In *International conference on machine learning*, pp. 12888–12900. PMLR, 2022.

Junnan Li, Dongxu Li, Silvio Savarese, and Steven Hoi. Blip-2: Bootstrapping language-image pre-training with frozen image encoders and large language models. In *International conference on machine learning*, pp. 19730–19742. PMLR, 2023.

Zhenwen Liang, Tianyu Yang, Jipeng Zhang, and Xiangliang Zhang. Unimath: A foundational and multimodal mathematical reasoner. In *Proceedings of the 2023 Conference on Empirical Methods in Natural Language Processing*, pp. 7126–7133, 2023.

Hunter Lightman, Vineet Kosaraju, Yura Burda, Harri Edwards, Bowen Baker, Teddy Lee, Jan Leike, John Schulman, Ilya Sutskever, and Karl Cobbe. Let's verify step by step. *arXiv preprint arXiv:2305.20050*, 2023.

Haotian Liu, Chunyuan Li, Yuheng Li, Bo Li, Yuanhan Zhang, Sheng Shen, and Yong Jae Lee. Llava-next: Improved reasoning, ocr, and world knowledge (january 2024). *URL https://llava-vl. github. io/blog/2024-01-30-llava-next*, 1(8).

Haotian Liu, Chunyuan Li, Yuheng Li, and Yong Jae Lee. Improved baselines with visual instruction tuning. In *Proceedings of the IEEE/CVF Conference on Computer Vision and Pattern Recognition*, pp. 26296–26306, 2024a.

Haotian Liu, Chunyuan Li, Qingyang Wu, and Yong Jae Lee. Visual instruction tuning. *Advances in neural information processing systems*, 36, 2024b.

Jiasen Lu, Dhruv Batra, Devi Parikh, and Stefan Lee. Vilbert: Pretraining task-agnostic visiolinguistic representations for vision-and-language tasks. *Advances in neural information processing systems*, 32, 2019.

Pan Lu, Ran Gong, Shibiao Jiang, Liang Qiu, Siyuan Huang, Xiaodan Liang, and Song-Chun Zhu. Inter-gps: Interpretable geometry problem solving with formal language and symbolic reasoning. *arXiv preprint arXiv:2105.04165*, 2021.

Pan Lu, Hritik Bansal, Tony Xia, Jiacheng Liu, Chunyuan Li, Hannaneh Hajishirzi, Hao Cheng, Kai-Wei Chang, Michel Galley, and Jianfeng Gao. Mathvista: Evaluating mathematical reasoning of foundation models in visual contexts. *arXiv preprint arXiv:2310.02255*, 2023.

Haipeng Luo, Qingfeng Sun, Can Xu, Pu Zhao, Jianguang Lou, Chongyang Tao, Xiubo Geng, Qingwei Lin, Shifeng Chen, and Dongmei Zhang. Wizardmath: Empowering mathematical reasoning for large language models via reinforced evol-instruct. *arXiv preprint arXiv:2308.09583*, 2023.

Ahmed Masry, Do Xuan Long, Jia Qing Tan, Shafiq Joty, and Enamul Hoque. Chartqa: A benchmark for question answering about charts with visual and logical reasoning. *arXiv preprint arXiv:2203.10244*, 2022.

Arindam Mitra, Hamed Khanpour, Corby Rosset, and Ahmed Awadallah. Orca-math: Unlocking the potential of slms in grade school math. *arXiv preprint arXiv:2402.14830*, 2024.

OpenAI. Gpt-4v(ision) system card. In *technical report*, 2023. URL `https://api.semanticscholar.org/CorpusID:263218031`.

Long Ouyang, Jeffrey Wu, Xu Jiang, Diogo Almeida, Carroll Wainwright, Pamela Mishkin, Chong Zhang, Sandhini Agarwal, Katarina Slama, Alex Ray, et al. Training language models to follow instructions with human feedback. *Advances in neural information processing systems*, 35:27730–27744, 2022.

Alec Radford, Jong Wook Kim, Chris Hallacy, Aditya Ramesh, Gabriel Goh, Sandhini Agarwal, Girish Sastry, Amanda Askell, Pamela Mishkin, Jack Clark, et al. Learning transferable visual models from natural language supervision. In *International conference on machine learning*, pp. 8748–8763. PMLR, 2021.

Zhihong Shao, Peiyi Wang, Qihao Zhu, Runxin Xu, Junxiao Song, Mingchuan Zhang, YK Li, Yu Wu, and Daya Guo. Deepseekmath: Pushing the limits of mathematical reasoning in open language models. *arXiv preprint arXiv:2402.03300*, 2024.

Wenhao Shi, Zhiqiang Hu, Yi Bin, Junhua Liu, Yang Yang, See-Kiong Ng, Lidong Bing, and Roy Ka-Wei Lee. Math-llava: Bootstrapping mathematical reasoning for multimodal large language models, 2024.

Shaden Smith, Mostofa Patwary, Brandon Norick, Patrick LeGresley, Samyam Rajbhandari, Jared Casper, Zhun Liu, Shrimai Prabhumoye, George Zerveas, Vijay Korthikanti, et al. Using deepspeed and megatron to train megatron-turing nlg 530b, a large-scale generative language model. *arXiv preprint arXiv:2201.11990*, 2022.

Hao Tan and Mohit Bansal. Lxmert: Learning cross-modality encoder representations from transformers. *arXiv preprint arXiv:1908.07490*, 2019.

Gemini Team, Rohan Anil, Sebastian Borgeaud, Yonghui Wu, Jean-Baptiste Alayrac, Jiahui Yu, Radu Soricut, Johan Schalkwyk, Andrew M Dai, Anja Hauth, et al. Gemini: a family of highly capable multimodal models. *arXiv preprint arXiv:2312.11805*, 2023.

GLM Team, Aohan Zeng, Bin Xu, Bowen Wang, Chenhui Zhang, Da Yin, Diego Rojas, Guanyu Feng, Hanlin Zhao, Hanyu Lai, et al. Chatglm: A family of large language models from glm-130b to glm-4 all tools. *arXiv e-prints*, pp. arXiv–2406, 2024.

Hugo Touvron, Thibaut Lavril, Gautier Izacard, Xavier Martinet, Marie-Anne Lachaux, Timothée Lacroix, Baptiste Rozière, Naman Goyal, Eric Hambro, Faisal Azhar, et al. Llama: Open and efficient foundation language models. *arXiv preprint arXiv:2302.13971*, 2023a.

Hugo Touvron, Louis Martin, Kevin Stone, Peter Albert, Amjad Almahairi, Yasmine Babaei, Nikolay Bashlykov, Soumya Batra, Prajjwal Bhargava, Shruti Bhosale, et al. Llama 2: Open foundation and fine-tuned chat models. *arXiv preprint arXiv:2307.09288*, 2023b.

Ke Wang, Houxing Ren, Aojun Zhou, Zimu Lu, Sichun Luo, Weikang Shi, Renrui Zhang, Linqi Song, Mingjie Zhan, and Hongsheng Li. Mathcoder: Seamless code integration in llms for enhanced mathematical reasoning. *arXiv preprint arXiv:2310.03731*, 2023a.

Ke Wang, Junting Pan, Weikang Shi, Zimu Lu, Mingjie Zhan, and Hongsheng Li. Measuring multimodal mathematical reasoning with math-vision dataset. *arXiv preprint arXiv:2402.14804*, 2024.

Peiyi Wang, Lei Li, Zhihong Shao, RX Xu, Damai Dai, Yifei Li, Deli Chen, Y Wu, and Zhifang Sui. Math-shepherd: Verify and reinforce llms step-by-step without human annotations. *CoRR, abs/2312.08935*, 2023b.

Weihan Wang, Qingsong Lv, Wenmeng Yu, Wenyi Hong, Ji Qi, Yan Wang, Junhui Ji, Zhuoyi Yang, Lei Zhao, Xixuan Song, et al. Cogvlm: Visual expert for pretrained language models. *arXiv preprint arXiv:2311.03079*, 2023c.

Jason Wei, Xuezhi Wang, Dale Schuurmans, Maarten Bosma, Fei Xia, Ed Chi, Quoc V Le, Denny Zhou, et al. Chain-of-thought prompting elicits reasoning in large language models. *Advances in neural information processing systems*, 35:24824–24837, 2022.

Zhen Yang, Ming Ding, Qingsong Lv, Zhihuan Jiang, Zehai He, Yuyi Guo, Jinfeng Bai, and Jie Tang. Gpt can solve mathematical problems without a calculator. *arXiv preprint arXiv:2309.03241*, 2023.

Qinghao Ye, Haiyang Xu, Guohai Xu, Jiabo Ye, Ming Yan, Yiyang Zhou, Junyang Wang, Anwen Hu, Pengcheng Shi, Yaya Shi, et al. mplug-owl: Modularization empowers large language models with multimodality. *arXiv preprint arXiv:2304.14178*, 2023.

Huaiyuan Ying, Shuo Zhang, Linyang Li, Zhejian Zhou, Yunfan Shao, Zhaoye Fei, Yichuan Ma, Jiawei Hong, Kuikun Liu, Ziyi Wang, et al. Internlm-math: Open math large language models toward verifiable reasoning. *arXiv preprint arXiv:2402.06332*, 2024.

Longhui Yu, Weisen Jiang, Han Shi, Jincheng Yu, Zhengying Liu, Yu Zhang, James T Kwok, Zhenguo Li, Adrian Weller, and Weiyang Liu. Metamath: Bootstrap your own mathematical questions for large language models. *arXiv preprint arXiv:2309.12284*, 2023.

Zheng Yuan, Hongyi Yuan, Chengpeng Li, Guanting Dong, Chuanqi Tan, and Chang Zhou. Scaling relationship on learning mathematical reasoning with large language models. *arXiv preprint arXiv:2308.01825*, 2023.

Xiang Yue, Xingwei Qu, Ge Zhang, Yao Fu, Wenhao Huang, Huan Sun, Yu Su, and Wenhu Chen. Mammoth: Building math generalist models through hybrid instruction tuning. *arXiv preprint arXiv:2309.05653*, 2023.

Xiang Yue, Yuansheng Ni, Kai Zhang, Tianyu Zheng, Ruoqi Liu, Ge Zhang, Samuel Stevens, Dongfu Jiang, Weiming Ren, Yuxuan Sun, et al. Mmmu: A massive multi-discipline multimodal understanding and reasoning benchmark for expert agi. In *Proceedings of the IEEE/CVF Conference on Computer Vision and Pattern Recognition*, pp. 9556–9567, 2024a.

Xiang Yue, Tuney Zheng, Ge Zhang, and Wenhu Chen. Mammoth2: Scaling instructions from the web. *arXiv preprint arXiv:2405.03548*, 2024b.

Aohan Zeng, Xiao Liu, Zhengxiao Du, Zihan Wang, Hanyu Lai, Ming Ding, Zhuoyi Yang, Yifan Xu, Wendi Zheng, Xiao Xia, et al. Glm-130b: An open bilingual pre-trained model. *arXiv preprint arXiv:2210.02414*, 2022.

Renrui Zhang, Dongzhi Jiang, Yichi Zhang, Haokun Lin, Ziyu Guo, Pengshuo Qiu, Aojun Zhou, Pan Lu, Kai-Wei Chang, Peng Gao, et al. Mathverse: Does your multi-modal llm truly see the diagrams in visual math problems? *arXiv preprint arXiv:2403.14624*, 2024.

Zhuosheng Zhang, Aston Zhang, Mu Li, Hai Zhao, George Karypis, and Alex Smola. Multimodal chain-of-thought reasoning in language models. *arXiv preprint arXiv:2302.00923*, 2023.

Deyao Zhu, Jun Chen, Xiaoqian Shen, Xiang Li, and Mohamed Elhoseiny. Minigpt-4: Enhancing vision-language understanding with advanced large language models. *arXiv preprint arXiv:2304.10592*, 2023.

A Dataset Cases

In this section, we provide a detailed overview of specific cases from our constructed MathVL dataset. These cases demonstrate the variety of mathematical disciplines covered by MathVL, including arithmetic, geometry, algebra, statistics, and word problems. Figure 7, Figure 8, Figure 9, Figure 10, and Figure 11 depict the types of problems that MathGLM-Vision is designed to tackle in each respective category. Each of these categories is critical for assessing the comprehensive mathematical capabilities of MathGLM-Vision. By tackling a wide range of problems, MathGLM-Vision demonstrates its versatility and robustness in addressing diverse mathematical tasks.

B Backbone Models

We utilize the following multi-modal large language models as our backbone models for conducting Specialized Fine-Tuning (SFT) on the constructed MathVL. The detailed description of each backbone model can be represented as follows:

- **GLM-4V-9B** is a bilingual (Chinese and English) multi-modal large language model, developed collaboratively by Zhipu.AI and Tsinghua University. It is built upon the foundational architecture of GLM-4-9B, enhancing its capabilities to handle complex multi-modal interactions. GLM-4V-9B takes a high resolution of 1120 * 1120 images as visual inputs. In comprehensive evaluations that test various capabilities including combined language skills, perceptual reasoning, text recognition, and chart understanding, GLM-4V-9B consistently outperforms competitors such as GPT-4-turbo-2024-04-09, Gemini 1.0 Pro, Qwen-VL-Max, and Claude 3 Opus, demonstrating its superior performance across multiple modalities.
- **CogVLM2** is a series of open-source multi-modal large language models derived from Meta-Llama-3-8B-Instruct, developed by Zhipu.AI and Tsinghua University. This series contains two models: cogvlm-llama3-chat-19B and cogvlm2-llama3-chinese-chat-19B. The former is a monolingual language model focused on English and the latter is a bilingual model supporting both English and Chinese. CogVLM2 is designed to handle extended content lengths up to 8K and accepts high-resolution images up to 1344 * 1344. Here, we choose cogvlm2-llama3-chinese-chat-19B as our backbone to pre-train our MathGLM-Vision-19B.
- **CogVLM-32B** is a close-source multi-modal large language model, developed by Zhipu.AI and Tsinghua University. It is based on the GLM-32B architecture and is optimized for handling complex multi-modal tasks. CogVLM-32B is engineered to process visual inputs at a high resolution of 1120 * 1120, enabling detailed image analysis and enhanced interaction with visual data.

Table 8 demonstrates an overview of the MathGLM-Vision series, detailing the different model parameters and configurations.

Model	LLM Size	ToTal Size	Language Model			Image Encoder		
			Layers	Hidden Size	Heads	Layers	Hidden Size	Heads
MathGLM-Vision-9B	9B	20B	40	4096	32	63	1792	16
MathGLM-Vision-19B	8B	19B	32	4096	32	63	1792	16
MathGLM-Vision-32B	32B	43B	58	6656	52	63	1792	16

Table 8: An overview of MathGLM-Vision series along with model parameters and configurations.

C Descriptions of VQA Datasets

Here, we provide a detailed description of collected visual question answering datasets (VQA) datasets. Table 9 demonstrates details 19 different VQA datasets, including task types and visual context.

Question

Given that a, b, and c are points on the number line as shown in the figure, simplify |a - b| - 2|c - b| + |b - c| to get _____.

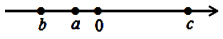

Answer

[Solution]Given that from the figure, b < a < 0 < c, we have a - b > 0 and b - c < 0. Therefore, the original expression simplifies to a - b - 2(c - b) - b + c = a - c.
[Answer]The answer is a - c.

Question

According to the program flow shown in the figure, if the initial input value is x = 4, the final output result is ( )
A. 60 B. 1540 C. 1500 D. 2020

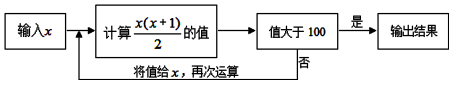

Answer

[Solution] Substitute x = 4 into the program flow: (4 × (4 + 1)) / 2 = 10, which is less than 100. Substitute x = 10 into the program flow: (10 × (10 + 1)) / 2 = 55, which is less than 100. Substitute x = 55 into the program flow: (55 × (55 + 1)) / 2 = 1540, which is greater than 100. Therefore, the final output result is 1540.
[Answer]The answer is B.

Question

As shown in the figure, in the long division of 28 by 16, the step indicated by the arrow represents ( )
A. 80 ones B. 80 tenths C. 80 hundredths

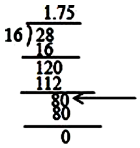

Answer

[Solution]The 8 indicated by the arrow is in the tenths place, and after dropping the 0, it combines with 8 to form 80 hundredths; based on this, the solution can be given. In the long division of 28 by 16, the step indicated by the arrow represents 80 hundredths.
[Answer]The answer is C.

Question

Given that the positions of numbers a and b on the number line are as shown in the figure, then a + b is ( )
A. Negative B. Positive C. 0 D. Indeterminate.

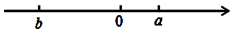

Answer

[Solution]Given that b < 0 < a and |a| < |b|, therefore, a + b < 0. Thus, a + b is a negative number. So the answer is A. From the given conditions, we know b < 0 < a and |a| < |b|, which leads to the conclusion. This problem tests the understanding of the number line. Using the number line to determine the relationship between a and b is key to solving the problem.
[Answer] A

Question

As shown in the figure, below is Yutan's test paper. The score is ( )
A. 20 points B. 80 points C. 0 points D. 40 points

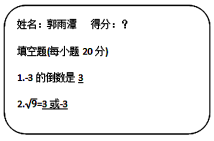

Answer

[Solution]The reciprocal of -3 is -1/3, so the first question is incorrect. The arithmetic square root of √9 is 3, so the second question is incorrect. Therefore, Yutan's score is 0 points. Thus, the answer is C. First, according to the rule of finding the reciprocal of an integer, which is one over that integer, the reciprocal of -3 is -1/3. Then, according to the definition and method of finding the arithmetic square root, the arithmetic square root of √9 is 3. This problem mainly tests the understanding and method of finding the arithmetic square root and the reciprocal, which should be mastered well.
[Answer]C.

Figure 7: Cases of arithmetical problems in our MathVL dataset.

Question

As shown in the figure, it is known that BC is parallel to GE, and ∠AFG = ∠1 = 50°.
(1) Prove that AF is parallel to DE;
(2) If AQ bisects ∠FAC, intersects BC at point Q, and ∠Q = 15°, find the measure of ∠ACQ.

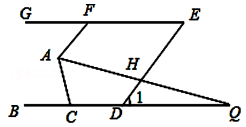

Answer

[Solution](1) According to the properties of parallel lines, we get ∠E = ∠1 = 50°. Given that ∠AFG = 50°, we have ∠AFG = ∠E. Finally, according to the criteria for parallel lines, we can draw the conclusion. (2) According to the properties of the exterior angle of a triangle, we get ∠AHD = 65°. Using the properties of parallel lines and angle bisectors, we find ∠CAQ = 65°. By using the sum of the interior angles of a triangle, we can get the conclusion. This question tests the determination and properties of parallel lines, the definition of angle bisectors, and the properties of the exterior angle of a triangle. Mastery of the determination and properties of parallel lines is key to solving the problem.
[Answer] (1) Proof: ∵ BC ∥ GE, ∴ ∠E = ∠1 = 50°, ∵ ∠AFG = ∠1 = 50°, ∴ ∠E = ∠AFG = 50°, ∴ AF ∥ DE; (2) Solution: ∵ ∠1 = 50°, ∠Q = 15°, ∴ ∠AHD = 65°, ∵ AF ∥ DE, ∴ ∠FAQ = ∠AHD = 65°, ∵ AQ bisects ∠FAC, ∴ ∠CAQ = ∠FAQ = 65°, ∴ ∠ACQ = 180° - ∠CAQ - ∠Q = 180° - 65° - 15° = 100°.

Question

As shown in the figure, in the equilateral triangle ABC, angle ∠C is cut along the dashed line DE. Then, ∠ADE + ∠DEB = _____.

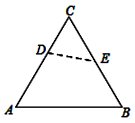

Answer

[Solution] Given that △ABC is an equilateral triangle, ∠A = ∠B = 60°. Therefore, ∠ADE + ∠BED = 360° - 60° × 2 = 240°. Thus, the answer is 240°. By first noting that ∠A and ∠B are each 60° due to the properties of an equilateral triangle, and then using the fact that the sum of the interior angles of a quadrilateral is 360°, subtracting the measures of ∠A and ∠B gives the result. This problem mainly tests the understanding of the interior angles of polygons and the properties of equilateral triangles, with the key point being that the sum of the interior angles of a quadrilateral is 360°.
[Answer] 240°.

Question

As shown in the figure, the large rectangle is composed of 2 identical large squares, 2 identical small squares, and 5 identical small rectangles. If the perimeter of this large rectangle is 48 cm, and the sum of the areas of the four squares is 68 cm^2, find the area of one of the small rectangles.

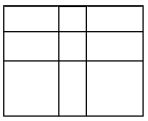

Answer

[Solution] Let the length of the small rectangle be a cm and the width be b cm. According to the problem, we have $a + b = 8$ and $a^2 + b^2 = 34$. Therefore, $ab = (1/2)[(a + b)^2 - (a^2 + b^2)] = 15$.
[Answer] The area of the small rectangle is 15 cm^2.

Question

As shown in the figure, the quadrilateral paper piece ABCD is folded along MN, and points A and D fall on A_1 and D_1 respectively. If ∠1 + ∠2 = 145°, then ∠B + ∠C = _____°.

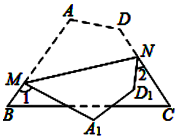

Answer

[Solution]Given that ∠1 + ∠2 = 145°, we have ∠AMN + ∠DNM = (360° - 145°) / 2 = 107.5°. Since ∠A + ∠D + (∠AMN + ∠DNM) = 360° and ∠A + ∠D + (∠B + ∠C) = 360°, it follows that ∠B + ∠C = ∠AMN + ∠DNM = 107.5°.
[Answer]The answer is 107.5°.

Question

The three views of a geometric body are shown in the figure. The surface area of the geometric body is ( )
A. 24 + 3π/4 B. 24 + 5π/4 C. 24 + π D. 8 + 3π/4

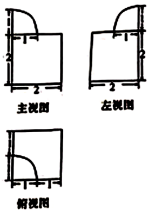

Answer

[Solution]Based on the three views of the geometric body, the geometric body is composed of a cube and an eighth of a sphere. Therefore, the surface area is $S = 6 \times 4 + (1/8) \times 4\pi \times 1^2 + (1/4) \times \pi \times 1^2 = 24 + 3\pi/4$.
[Answer] The answer is A.

Figure 8: Cases of geometric problems in our MathVL dataset.

Question

In the same Cartesian coordinate system, the graphs of the linear function $y = k_1x + b$ and the proportional function $y = k_2x$ are shown in the figure. The range of x values that satisfy $k_1x + b > k_2x$ is _____.

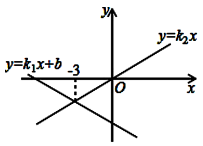

Answer

[Solution]When $x \leq -3$, the line l_1: $y_1 = k_1x + b$ is above the line l_2: $y_2 = k_2x$, meaning $k_1x + b > k_2x$. Therefore, the range of x values that satisfy $k_1x + b > k_2x$ is $x < -3$.
[Answer]The answer is $x < -3$.

Question

As shown in the figure, the graph represents the quadratic function $y = ax^2 + bx + c$. Among the following statements: ① $ac > 0$; ② $a - b + c < 0$; ③ $4ac < b^2$; ④ $2a + b > 0$; ⑤ When $x > 0$, y decreases as x increases. The number of correct statements is ( )
A. 1 B. 2 C. 3 D. 4

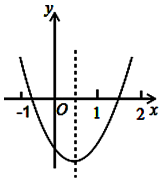

Answer

[Solution]① From the graph, we know that $a > 0$ and $c < 0$, so $ac < 0$. Thus, ① is incorrect. ② From the graph, we know that when $x = -1$, $y = a - b + c > 0$, so ② is incorrect. ③ Since the parabola has two intersection points with the x-axis, $\triangle = b^2 - 4ac > 0$. Thus, ③ is correct. ④ From the axis of symmetry, we know that $-b / 2a < 1$, so $2a + b > 0$. Thus, ④ is correct. ⑤ When $x > -b / 2a$, y increases as x increases, so ⑤ is incorrect.
[Answer]The answer is B.

Question

The graph of the quadratic function $y = ax^2 + bx + c$ is shown in the figure. Among the following conclusions: ① $ab > 0$; ② $a + b - 1 = 0$; ③ $a > 1$; ④ One root of the quadratic equation $ax^2 + bx + c = 0$ is 1, and the other root is $-1/a$. The correct conclusions are _____.

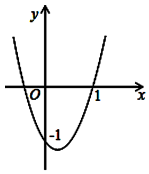

Answer

[Solution]① From the graph of the quadratic function, we know that the parabola opens upwards, so $a > 0$. The axis of symmetry is to the right of the y-axis, so $b < 0$. Therefore, $ab < 0$, making ① incorrect. ② From the graph, we know that the parabola intersects the x-axis at (1, 0) and the y-axis at (0, -1). Therefore, $c = -1$ and $a + b - 1 = 0$, making ② correct. ③ Since $a + b - 1 = 0$, we have $a - 1 = -b$. Given that $b < 0$, we have $a - 1 > 0$, so $a > 1$, making ③ correct. ④ Since the parabola intersects the y-axis at (0, -1), the equation of the parabola is $y = ax^2 + bx - 1$. Since the parabola intersects the x-axis at (1, 0), one root of $ax^2 + bx - 1 = 0$ is 1. According to the relationship between the roots and coefficients, the other root is $-1/a$, making ④ correct.
[Answer]The correct conclusions are ②, ③, and ④.

Question

As shown in the figure, the solution set of the inequality $2x - a < -1$ is represented. The value of a is ( )
A. $a \leq -1$ B. $a \leq -2$ C. $a = -1$ D. $a = -2$

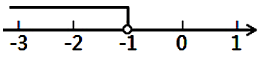

Answer

[Solution]Given $2x - a < -1$, we have $2x < a - 1$, which means $x < (a - 1) / 2$. From the number line, we know $x < -1$. Therefore, $(a - 1) / 2 = -1$. Solving this, we get $a = -1$.
[Answer]The answer is C.

Question

The store purchased a batch of T-shirts at a unit price of 20 yuan. After a trial sale, it was found that the daily sales volume y (units) and the sales price x (yuan/unit) satisfy the linear function relationship shown in the figure. (1) Find the function relationship between y and x (no need to write the range of x values). (2) Without considering factors like inventory, at what sales price will the daily profit W be maximized?

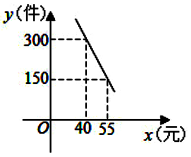

Answer

[Solution](1) Let the function relationship between y and x be $y = kx + b$ ($k \neq 0$). Substituting (40, 300) and (55, 150) into the equation, we get: $300 = 40k + b$ and $150 = 55k + b$. Solving, we get: $k = -10$ and $b = 700$. Therefore, the function relationship between y and x is $y = -10x + 700$. (2) From the problem, we get: $W = (x - 20) \cdot y = (x - 20)(-10x + 700) = -10x^2 + 900x - 14000 = -10(x - 45)^2 + 6250$. Since $-10 < 0$, when $x = 45$, W reaches its maximum value of 6250 yuan.
[Answer]Without considering factors like inventory, the daily profit W is maximized when the sales price is set at 45 yuan.

Figure 9: Cases of algebraic problems in our MathVL dataset.

Question

A city plans to build a flower bed in the central square, dividing it into 6 parts (as shown in the figure). Four different colors of flowers need to be planted, one color per part, and adjacent parts cannot have the same color. The number of different planting methods is _____. (Answer with a number)

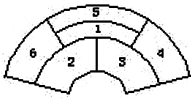

Answer

[Solution]From the problem's context, we need to plant flowers of 4 different colors in 6 parts. From the figure, we can see that there must be 2 pairs of parts with the same color. We can classify and calculate the planting methods based on the parts with the same color. (1) If parts ② and ⑤ are the same color, then parts ③ and ⑥ or parts ④ and ⑥ must also be the same color. Therefore, the number of methods for this case is $N_1 = 4 \times 3 \times 2 \times 2 \times 1 = 48$. (2) If parts ③ and ⑤ are the same color, then parts ② and ④ or parts ⑥ and ④ must also be the same color. Therefore, the number of methods for this case is $N_2 = 4 \times 3 \times 2 \times 2 \times 1 = 48$. (3) If parts ② and ④ and parts ③ and ⑥ are the same color, then the number of methods for this case is $N_3 = 4 \times 3 \times 2 \times 1 = 24$. Therefore, the total number of planting methods is $N = N_1 + N_2 + N_3 = 48 + 48 + 24 = 120$.
[Answer]The answer is 120.

Question

In a shooting competition, Person A and Person B each shoot 5 times. The bar chart of their scores is shown in the figure. The number of correct statements among the following four is ( ) ① The mean of Person A's scores is equal to the mean of Person B's scores. ② The median of Person A's scores is greater than the median of Person B's scores. ③ The variance of Person A's scores is less than the variance of Person B's scores. ④ The range of Person A's scores is equal to the range of Person B's scores.
A. 1 B. 2 C. 3 D. 4

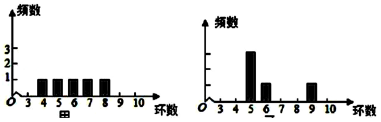

Answer

[Solution]In statement ①, the mean score for Person B is $(5 + 5 + 5 + 6 + 9) / 5 = 6$, and the mean score for Person A is $(4 + 5 + 6 + 7 + 8) / 5 = 6$. Therefore, the mean score for Person A is equal to the mean score for Person B, so ① is correct. In statement ②, the median score for Person A is 6, and the median score for Person B is 5. Therefore, the median score for Person A is greater than the median score for Person B, so ② is correct. In statement ③, the variance for Person A's scores is $(2^2 \times 2 + 1^2 \times 2) / 5 = 2$, and the variance for Person B's scores is $(1^2 \times 3 + 3^2 \times 1) / 5 = 2.4$. Therefore, the variance for Person A's scores is less than the variance for Person B's scores, so ③ is correct. In statement ④, the range for Person A's scores is 4, and the range for Person B's scores is 4. Therefore, the range for Person A's scores is equal to the range for Person B's scores, so ④ is correct.
[Answer]The answer is D.

Question

To understand the physical fitness of ninth-grade students at a certain school, a random sample of ninth-grade students was tested for the number of sit-ups they could do in one minute. The results were displayed in the histogram shown. Based on the chart, calculate the percentage of students whose number of sit-ups falls within the range of 25 to 30. The percentage is ( )
A. 40% B. 30% C. 20% D. 10%

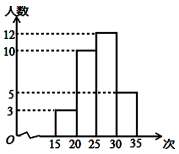

Answer

[Solution]From the frequency histogram, we can determine that the total number of students surveyed is 3 + 10 + 12 + 5 = 30. The number of students who did 25 to 30 sit-ups is 12, so the percentage is 40%.
[Answer]A.

Question

As shown in the pie chart, the number of seventh-grade (Class 1) students participating in extracurricular activities at a certain school is represented. If the number of students participating in art activities is 16, then the number of students participating in sports activities is _____.

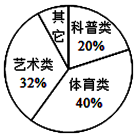

Answer

[Solution]Given that the number of seventh-grade (Class 1) students participating in art activities is 16, which represents 32% of the total number of students in the class, the total number of students in seventh-grade (Class 1) is $16 \div 32\% = 50$. Since the percentage of students participating in sports activities is 40%, the number of students participating in sports activities is $50 \times 40\% = 20$.
[Answer]The answer is 20.

Question

As shown in the chart regarding the weekly physical exercise of students in a certain class, the mode and median of the time spent on physical exercise by the students this week are ( )
A. 8, 9 B. 8, 8.5 C. 16, 8.5 D. 16, 14

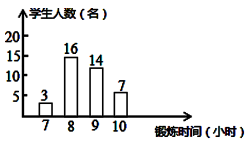

Answer

[Solution]The mode is the number that appears most frequently in a data set, which is 8. When the data set is arranged in ascending order, the number in the middle position is the median. According to the definition of median, the median of this data set is 9.
[Answer]The answer is A.

Figure 10: Cases of statistical problems in our MathVL dataset.

Question

During the May Day holiday, there was an appliance promotion, and mom bought two appliances as shown in the figure. (1) How much did mom spend in total? (2) How much cheaper was the microwave oven compared to its original price? (3) Can you propose and solve other math problems based on this scenario?

Answer

(1) 5900 yuan (2) 300 yuan (3) Question: How much cheaper was the washing machine compared to its original price? Answer: 1900 yuan

Question

As shown in the figure, the operating hours of Haichang Polar Ocean Park are (_____) hours.

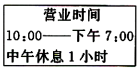

Answer

This question requires calculating the operating hours, which is the elapsed time. Using the formula elapsed time = end time - start time, convert 7 PM to 24-hour time as 19:00. Thus, 19:00 - 10:00 = 9 hours, then subtract a 1-hour lunch break. Therefore, the answer is 8 hours.

Question

The store is preparing to bag 120 apples for sale (as shown in the figure). The apples can be evenly divided into bags of (_____) apples each; using bags of (_____) apples each will leave (_____) apples remaining.

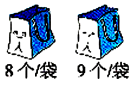

Answer

Divide 120 by 8 and 9 respectively to get the answer. 120 ÷ 8 = 15 (bags) 120 ÷ 9 = 13 (bags) with a remainder of 3 (apples) Therefore, 120 apples can be evenly divided into bags of 8 apples each, and when using bags of 9 apples each, there will be 3 apples remaining. So the answer is: 8, 9, 3.

Question

As shown in the figure, at the 15th Asian Games, China won ( ) more gold medals than the combined total of gold medals won by South Korea and Japan.
A. 108 B. 57 C. 115 D. 107

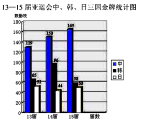

Answer

[Solution] 165 - (58 + 50) = 165 - 108 = 57 (medals) Thus, China won 57 more gold medals than the combined total of South Korea and Japan. [Answer] B

Question

Mr. Zhang and Mr. Ma took a taxi together from the school. Mr. Zhang went to Xinhua Bookstore, and Mr. Ma went to Yintai Department Store (as shown in the figure). They agreed to share the taxi fare reasonably. The taxi fare rates are: 0-3 kilometers (base fare) 10 yuan, and beyond 3 kilometers, 1.8 yuan per kilometer (rounded up to the nearest kilometer). Please help them calculate how much each person should pay.

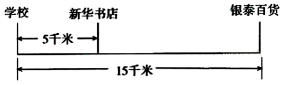

Answer

[Solution] 10 + (5 - 3) × 1.8 = 13.6 yuan 1.8 × (15 - 5) = 18 yuan 13.6 ÷ 2 = 6.8 yuan 6.8 + 18 = 24.8 yuan.Thus, Mr. Zhang should pay 6.8 yuan, and Mr. Ma should pay 24.8 yuan. [Answer] 6.8 yuan; 24.8 yuan.

Figure 11: Cases of word problems in our MathVL dataset.

Dataset	Task	Visual Context
DocVQA	Figure Question Answering (FQA)	Document Image
DVQA	Figure Question Answering (FQA)	Bar Chart
FigureQA	Figure Question Answering (FQA)	Charts and Plots
PlotQA	Figure Question Answering (FQA)	Bar, Line, Scatter
MapQA	Figure Question Answering (FQA)	Map Chart
IconQA	Math Word Problem (MWP)	Abstract Scene
TabMWP	Math Word Problem (MWP)	Table
CLEVR-Math	Math Word Problem (MWP)	Synthetic Scene
TQA	Textbook Question Answering (TQA)	Scientific Figure
AI2D	Textbook Question Answering (TQA)	Scientific Figure
ScienceQA	Textbook Question Answering (TQA)	Scientific Figure
A-OKVQA	Visual Question Answering (VQA)	Natural Image
VQA2.0	Visual Question Answering (VQA)	Natural Image
PMC-VQA	Visual Question Answering (VQA)	Medical Image
VizWiz	Visual Question Answering (VQA)	Natural Image
Super-CLEVR	Visual Question Answering (VQA)	Synthetic Scene
VQA-AS	Visual Question Answering (VQA)	Abstract Scene
VQA-RAD	Visual Question Answering (VQA)	Medical Image
TextVQA	Visual Question Answering (VQA)	Natural Image

Table 9: Summary of VQA datasets.

D Implementation Details

We provide a detailed overview of the Specialized Fine-Tuning (SFT) process applied to our MathGLM-Vision. The specific hyperparameters used during this process are outlined in Table 10.

parameters	MathGLM-Vision-9B	MathGLM-Vision-19B	MathGLM-Vision-32B
Total steps	35,000	35,000	35,000
Global Batch Size	128	128	128
Learning Rate	$1e^{-5}$	$1e^{-5}$	$1e^{-5}$
Learning Rate Schedule	cosine decay	cosine decay	cosine decay
Warmup Ratio	0.01	0.01	0.01
Weight Decay	$5e^{-2}$	$5e^{-2}$	$5e^{-2}$
Optimizer	AdamW	AdamW	AdamW
Input Resolution	1120 * 1120	1344 * 1344	1120 * 1120
Image Length	1600	2304	1600

Table 10: The detailed setup of the SFT procedures.

E The detailed description of Benchmark Datasets

In this section, we provide an in-depth description of the benchmark datasets used to evaluate the performance of MathGLM-Vision. These benchmark datasets have been carefully curated to test the MLLMs' capabilities. The detailed description of benchmark datasets is provides as follows.

- **MathVista**
  MathVista is a comprehensive benchmark dataset designed to rigorously evaluate the mathmetical reasoning capabilities of language models (LMs), especially in varied visual contexts.
  This dataset offers a comprehensive evaluation benchmark designed to integrate mathematical reasoning with visual understanding, focusing on five primary tasks: figure question

answering (FQA); geometry problem solving (GPS); math word problem (MWP); textbook question answering (TQA); and visual question answering (VQA).

- **MathVista-GPS**

  MathVista-GPS, a subset of the MathVista Dataset, specifically focuses on the domain of geometry problem solving. The questions in this subset range from basic shape recognition to more advanced problems involving theorems, calculations and reasoning.

- **MathVerse**

  MathVerse is designed to provide a fair and comprehensive assessment of MLLMs' capabilities in visual mathematics. The benchmark comprises 2,612 high-quality, multi-subject math problems, each featuring diagrams and converted into six different versions by human annotators. These versions offer varying levels of multi-modal information, allowing for a thorough evaluation of MLLMs' understanding of visual diagrams.

- **MATH-Vision**

  The MATH-Vision (MATH-V) dataset comprises 3,040 high-quality mathematical problems, each featuring a visual context and sourced from 19 real math competitions. This extensive and diverse collection allows for a comprehensive evaluation of LMMs' ability to interpret and reason with visual information in mathematical contexts.

- **MMMU**

  The Massive Multi-discipline Multi-modal Understanding and Reasoning (MMMU) benchmark encompasses 11.5K questions across six disciplines, including Art, Business, Health & Medicine, Science, Humanities & Social Science, and Tech & Engineering. The tasks in MMMU challenge models to perform sophisticated multi-modal analysis and apply domain-specific knowledge, demanding a higher level capability in comprehension and integration.

F Detailed Experimental Results on Public Benchmark Datasets

Results on the testmini subset of MathVista. To comprehensively evaluate the performance of MathGLM-Vision across various task types featured in the MathVista dataset, we systematically evaluate it on the testmini subset. This subset has been carefully selected to represent a diverse range of mathematical problem types, ensuring a robust assessment of our model's capabilities. Table 11 shows the evaluation results on the testmini subset of MathVista across various task types. Notably, MathGLM-Vision-19B and MathGLM-Vision-32B surpass human performance in overall accuracy, highlighting the advanced capabilities of these models in handling complex mathematical problems. In particular, MathGLM-Vision excels significantly in geometry problem solving (GPS) and geometry reasoning (GEO), demonstrating its superior proficiency in mathematical reasoning.

Model	Input	ALL	FQA	GPS	MWP	TQA	VQA	ALG	ARI	GEO	LOG	NUM	SCI	STA
Human Performance	Q, I	60.30	59.70	48.40	73.00	63.20	55.90	50.90	59.20	51.40	40.70	53.80	64.90	63.90
2-shot CoT GPT-4	Q, I_c, I_t	30.50	27.21	35.91	21.30	43.13	28.17	35.72	25.17	35.80	24.74	15.41	47.28	31.29
2-shot PoT GPT-4	Q, I_c, I_t	31.74	27.58	37.35	23.87	43.00	30.27	37.15	27.93	37.48	22.68	15.83	44.47	31.87
GPT-4V	Q, I	49.90	43.10	50.50	57.50	65.20	38.00	53.00	49.00	51.00	21.60	20.10	63.10	55.80
LLaVA-LLaMA-2-13B	Q, I	25.40	22.86	24.57	18.15	35.82	29.69	26.93	22.47	24.45	19.07	19.05	34.71	21.61
MathGLM-Vision-9B	Q, I	52.20	46.10	64.42	58.60	55.70	37.43	59.79	43.91	62.34	10.81	37.50	54.10	54.82
MathGLM-Vision-19B	Q, I	61.10	59.85	**65.38**	68.28	53.80	**55.31**	59.79	59.21	**63.18**	**18.92**	**59.03**	53.28	68.44
MathGLM-Vision-32B	Q, I	**62.40**	**62.83**	62.02	**69.35**	**62.03**	54.19	**60.50**	**60.62**	61.92	16.22	52.08	**60.66**	**72.09**

Table 11: **Accuracy scores on the *testmini* subset of MathVista.** Input: Q: question, I: image, I_c: image caption, I_t: OCR texts detected from the image. ALL: overall accuracy. Task types: FQA: figure question answering, GPS: geometry problem solving, MWP: math word problem, TQA: textbook question answering, VQA: visual question answering. Mathematical reasoning types: ALG: algebraic reasoning, ARI: arithmetic reasoning, GEO: geometry reasoning, LOG: logical reasoning, NUM: numeric common sense, SCI: scientific reasoning, STA: statistical reasoning. The highest accuracy among all baseline MLLMs is marked in red, while the highest accuracy among various variants of MathGLM-Vision is marked bold.

Results on the testmini set of MathVerse. To thoroughly evaluate the performance of MathGLM-Vision across 12 detailed subjects within the MathVerse dataset, we conduct comprehensive experiments and report the results in Table 12. This analysis delves into the model's ability to address a broad spectrum of mathematical challenges, ranging from geometry to functions. As shown in Table 12, MathGLM-Vision surpasses all open-source MLLMs and most close-source MLLMs. However, it still falls short by 14% compared to the performance of GPT-4V. In some subjects such as Angle, Analytic, and Property, MathGLM-Vision achieves better performance compared the advanced GPT-4V. For example, MathGLM-Vision-32B shows remarkable performance in plane geometry, particularly in handling angle-related problems, where it achieves a 60.1% accuracy, showcasing its strong geometric reasoning capabilities.

Model	All	Plane Geometry						Solid Geometry				Functions				
		All	Len	Area	Angle	Anal	Apply	All	Len	Area	Vol	All	Coord	Prop	Exp	Apply
Closed-source MLLMs																
Qwen-VL-Plus	21.3	17.3	19.1	16.4	16.1	23.6	13.2	24.8	18.1	18.7	33.4	31.3	52.5	25.1	10.8	50.3
Gemini-Pro	35.3	33.0	32.2	42.6	28.4	30.2	32.3	33.4	35.0	29.3	36.1	28.3	25.7	26.6	10.8	51.3
Qwen-VL-Max	37.2	38.4	41.7	46.4	32.6	40.6	38.7	33.7	25.4	28.3	42.6	38.4	43.7	35.5	13.6	61.0
GPT-4V	54.4	56.9	60.8	63.4	52.6	48.5	60.9	50.2	54.8	39.9	56.8	52.8	72.3	47.1	30.9	70.1
Open-source MLLMs																
LLaMA-Adapter V2	5.8	5.9	4.0	5.9	6.6	13.4	3.3	4.6	5.3	3.1	5.7	6.2	6.7	6.1	4.5	7.9
ImageBind-LLM	10.0	9.7	12.1	9.9	9.2	10.2	4.8	4.6	4.9	3.5	5.3	14.9	12.3	13.8	4.6	25.9
mPLUG-Owl2	10.3	7.7	8.2	6.0	5.7	12.4	10.6	11.0	9.2	6.7	15.7	17.4	22.8	18.6	5.3	22.2
MiniGPT-v2	10.9	11.6	10.0	9.8	14.3	9.1	11.8	1.7	2.2	1.6	0.5	11.2	4.2	15.7	4.0	21.1
LLaVA-1.5	12.7	11.8	13.1	15.1	9.7	9.4	13.2	10.6	12.1	8.7	11.6	14.8	18.8	12.7	9.5	23.7
SPHINX-Plus	14.0	14.4	14.2	10.5	14.1	16.5	16.8	7.0	7.2	6.1	7.6	17.9	11.1	19.1	6.3	27.7
G-LLaVA	15.7	20.2	17.3	13.6	26.5	5.9	23.1	5.0	10.3	4.4	3.1	9.2	9.1	9.1	1.3	15.5
LLaVA-NeXT	17.2	15.9	14.8	13.1	16.3	17.7	17.8	19.6	33.3	11.7	12.6	23.1	24.5	23.4	8.0	33.1
ShareGPT4V	17.4	16.9	16.2	17.9	16.9	12.2	21.1	15.0	13.6	10.9	19.7	20.2	19.9	22.2	8.4	25.8
SPHINX-MoE	22.8	24.5	26.3	28.4	21.1	26.6	24.4	15.8	9.4	10.7	26.3	19.5	23.5	19.3	9.2	30.3
InternLM-XC2	25.9	26.2	27.1	29.7	20.6	18.5	22.2	20.1	34.5	14.1	25.2	23.7	24.4	24.9	10.6	36.3
MathGLM-Vision																
MathGLM-Vision-9B	44.2	45.3	**43.7**	48.9	41.5	**53.5**	52.2	42.0	54.2	50.0	29.4	42.1	25.0	42.3	**43.8**	47.5
MathGLM-Vision-19B	42.5	41.8	34.8	**55.3**	38.9	46.5	**53.6**	**51.3**	**66.7**	**52.3**	**43.1**	38.4	18.8	38.0	28.1	55.0
MathGLM-Vision-32B	**49.2**	**49.0**	42.4	59.6	**51.3**	48.8	50.7	45.4	62.5	40.9	41.2	**52.8**	**43.8**	**59.2**	40.6	**55.0**

Table 12: **Mathematical Evaluation on Different Subjects and Subfields in MathVerse's *testmini* Set.** Len: Length; Anal: Analytic; Apply: Applied; Vol: Volume; Coord: Coordinate; Prop: Property; Exp: Expressio. The highest accuracy among all baseline MLLMs is marked in red, while the highest accuracy among various variants of MathGLM-Vision is marked bold.

Results on Math-Vision datasets. To effectively assess MathGLM-Vision's ability across diverse subjects and difficulty levels within the Math-Vision dataset, we conduct a series of detailed evaluation experiments and report results in Table 13. Specifically, GPT-4V leads the close-source models with an overall accuracy of 22.76%, yet it remains significantly below the human performance benchmark of 75.66%. MathGLM-Vision shows competitive performance across a variety of mathematical disciplines compared to most of close-source MLLMs, with MathGLM-Vision-32B achieving the overall accuracy of 26.5%, closely approaching that of GPT-4V. Notably, MathGLM-Vision-32B excels in solid geometry with a accuracy of 29.1%, significantly outperforming the accuracy of 23.8% on GPT-4V. This superior performance in solid geometry highlights MathGLM-Vision-32B's advanced spatial reasoning and geometric processing capabilities, which are essential for tackling complex three-dimensional problems.

G Error Cases

Figure 12, Figure 13, Figure 14, and Figure 15 show examples of errors made by MathGLM-Vision-32B on the MathVL-test dataset. Each figure highlights a specific type of error, providing valuable insights into the model's limitations and areas for improvement.

H Case Study

Figure 16, Figure 17, Figure 18, and Figure 19 present several case studies from MathGLM-Vision-32B. These figures showcase the model's performance in various scenarios, highlighting its strengths

Question

As shown in the figure, when a weight is placed in a measuring cup and water is added, the relationship between the height of the water in the cup (y) and the volume of water added (x) is approximately ( ).

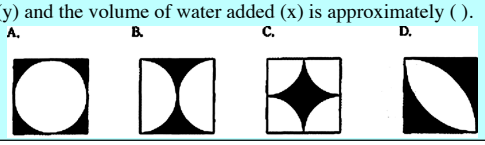

GT Answer: B

MathGLM-Vision-32B: Reasoning Error

Analysis: According to the problem, the relationship between the height of the water in the cup (y) and the volume of water added (x) should be divided into two segments: initially slow, then fast. Solution: Since a weight is placed in the cup first, the height of the water (y) initially increases slowly with the volume of water added (x). Only when the water surface surpasses the weight does the height increase rapidly with the addition of more water. Therefore, the answer is C.

Figure 12: **An example of reasoning error.** MathGLM-Vision-32B mistakenly believed that the height of the water would initially increase rapidly and then slowly, indicating a reasoning error.

Question

As shown in the figure, in the square paper ABCD, diagonals AC and BD intersect at point O. When the square paper is folded so that AD falls on BD, point A coincides with point F on BD. After unfolding, the crease DE intersects AB and AC at points E and G, respectively, and GF is connected. The following conclusions are correct:_____① $\angle AGD = 112.5°$; ② $S_{\triangle AGD} = S_{\triangle OGD}$; ③ the quadrilateral AEFG is a rhombus; ④ BE = 2OG.

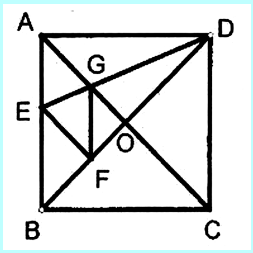

GT Answer: ①③④

MathGLM-Vision-32B: Vision Recognition Error

Problem analysis: ∵ The quadrilateral ABCD is a square, ∴ ∠BAD = 90°. Based on the folding properties: EF ⊥ AD, and AF = AB = AD. ∴ ∠EFA = ∠AED = 45°. ∴ AE ∥ GF. ∴ ∠AGF = ∠AGE = ∠GAB = 22.5°. ∴ ∠AGD = 180° - 22.5° × 3 = 112.5°. Therefore, statement ① is correct. It is easy to prove that △AEF ≅ △DFG (ASA). ∴ S_{△}{*AEF*} = *S*{△}{*DFG*}. ∴ *S*{△}{*AEF*} + *S*{△}{*OGF*} = *S*{△}{*OGF*} + *S*{△}{*OGD*}. ∴ *S*{△}{*AGD*} = *S*{△}_{OGD}. Therefore, statement ② is correct. From ①, we get AE ∥ GF, and AE = GF. ∴ The quadrilateral AEFG is a parallelogram. Furthermore, ∵ ∠EFA = 45°, ∴ ∠GEF = 67.5°. ∴ ∠AGE = 67.5°. ∴ AE = EG. ∴ The quadrilateral AEFG is a rhombus. Therefore, statement ③ is correct. Let OG = x, then BE = 2x. ∵ ∠OBE = ∠OBC + ∠CBE = 45° + 67.5° = 112.5°, ∠BOE = ∠BOC = 45°. ∴ ∠BEO = 180° - 112.5° - 45° = 22.5°. ∴ BE is not the height on the hypotenuse. ∴ BE ≠ 2OG. Therefore, statement ④ is incorrect. In conclusion, the correct statements are: ①②③.

Figure 13: **An example of vision recognition error.** MathGLM-Vision-32B incorrectly interpreted the geometric properties of the diagram, leading to a vision recognition error.

Question

As shown in Figure 1, in the isosceles trapezoid ABCD, AB ∥ CD, AD = BC, and DC = 2. A moving point P starts from point C and moves along CB and BA until it stops at point A. Let the distance traveled by point P be x, and the area of △DCP be y. If the graph of the function y with respect to x is shown in Figure 2, then the area of the isosceles trapezoid ABCD is ( ).

A. 12 B. 18 C. 20 D. 21

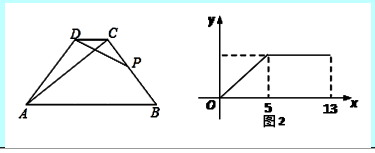

GT Answer: C

MathGLM-Vision-32B: Calculation Error

【Analysis】According to the graph of the function and the figure, we find the length of AB. Using the properties of the isosceles trapezoid, we find that DC = AD = BC = 2. Using the Pythagorean theorem, we find AC, and thus the answer.
【Solution】From the graph, we see that when point P moves 5 units, the area of △DCP starts to remain unchanged, so we deduce that BC = 5. As point P moves from C to B, y increases with x, and when x = 5, the area changes, so AB = 5. ∵ The quadrilateral ABCD is an isosceles trapezoid, ∴ ∠B = ∠BAD. Also, ∵ ∠B + ∠BAP = ∠BAD + ∠CDA, ∴ ∠CDA = ∠BAP. Also, ∵ ∠ADC = ∠BAP, ∴ △DCA ~ △PBA. Thus, CD : AB = DA : PA, which means 2 : 5 = (5 - 2) : PA. Solving for PA, we get PA = 3.75. ∴ The area of the isosceles trapezoid ABCD is the sum of the areas of △ABC and △DAB, which is 1/2 × (2 + 5) × 3.75 + 1/2 × 3.75 × 2 = 18.75 + 3.75 = 22.5. Therefore, the answer is D.

Figure 14: **An example of calculation error.** MathGLM-Vision-32B made an error in calculating the lengths and areas in the isosceles trapezoid, leading to an incorrect solution.

Question

As shown in the figure, the plane development diagram of a cube is given. In the cube, the positional relationship between AB and CD is ( )

A. Intersecting B. Parallel

C. Skew and Perpendicular D. Skew but not Perpendicular

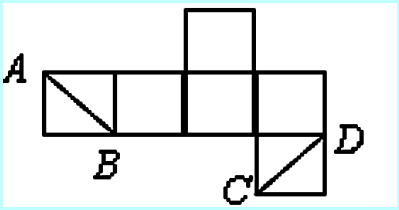

GT Answer: D

MathGLM-Vision-32B: Premature Conclusion Error

【Analysis】Utilize the characteristics of the cube and its unfolded surface diagram to solve the problem. 【Solution】This is a plane development diagram of a cube, with a total of six faces. Among them, face "A" is opposite to face "C," face "B" is opposite to face "D," and "AB" and "CD" are skew lines, and "AB ⊥ CD." Therefore, the answer is C.

Figure 15: **An example of premature conclusion error.** MathGLM-Vision-32B prematurely concluded that AB is perpendicular to CD without proper reasoning, leading to a premature conclusion error.

Model	Overall	Alg	AnaG	Ari	CombG	Comb	Cnt	DescG	GrphT	Log	Angle	Area	Len	SolG	Stat	Topo	TransG
Human Performance																	
Human (testmini)	75.66	57.9	79.0	100.0	100.0	47.4	94.7	89.5	63.2	63.2	36.8	52.6	73.7	89.5	89.5	100.0	73.7
Open-source MLLMs																	
LLaVA-v1.5-7B	8.52	7.0	7.1	10.7	7.1	4.8	10.5	7.7	10.0	9.2	15.6	10.2	9.8	5.3	8.6	4.4	4.8
SPHINX (V2)	9.70	6.7	7.1	12.9	7.5	7.7	6.0	9.6	16.7	10.1	11.0	11.8	12.5	8.2	8.6	8.7	6.0
ShareGPT4V-7B	10.53	5.5	3.6	12.9	10.1	4.8	7.5	11.5	14.4	10.9	16.2	11.8	12.3	9.8	15.5	17.4	11.3
LLaVA-v1.5-13B	11.12	7.0	14.3	14.3	9.1	6.6	6.0	13.5	5.6	13.5	10.4	12.6	14.7	11.5	13.8	13.0	10.7
ShareGPT4V-13B	11.88	7.5	15.5	16.4	10.7	8.9	9.0	11.5	8.9	7.6	11.6	13.0	17.4	10.3	8.6	8.7	12.5
SPHINX-MoE	14.18	7.8	17.9	14.3	15.6	9.5	11.9	12.5	15.6	12.6	16.2	15.6	17.8	13.5	12.1	8.7	16.1
InternLM-XComposer2-VL	14.54	9.3	15.5	12.1	15.3	11.3	10.5	14.4	22.2	19.3	19.7	15.6	15.0	11.9	15.5	26.1	15.5
Closed-source MLLMs																	
Qwen-VL-Plus	10.72	11.3	17.9	14.3	12.7	4.8	10.5	15.4	8.9	14.3	11.6	6.4	10.0	14.3	6.9	8.7	11.31
Qwen-VL-Max	15.59	10.7	19.1	20.0	16.9	12.5	17.9	16.4	12.2	21.0	13.3	14.2	19.8	11.5	20.7	13.0	17.3
Gemini Pro	17.66	15.1	10.7	20.7	20.1	11.9	7.5	20.2	21.1	16.8	19.1	19.0	20.0	14.3	13.8	17.4	20.8
GPT4V	22.76	27.3	32.1	35.7	21.1	16.7	13.4	22.1	14.4	16.8	22.0	22.2	20.9	23.8	24.1	21.7	25.6
MathGLM-Vision																	
MathGLM-Vision-9B	19.2	18.6	20.2	19.3	15.3	18.5	20.9	26.0	18.9	15.1	23.1	20.4	18.3	23.8	19.0	17.4	14.3
MathGLM-Vision-19B	21.6	22.0	**29.8**	23.6	22.4	18.5	**25.4**	25.0	17.8	16.0	20.2	22.0	20.3	21.3	20.7	**30.4**	23.2
MathGLM-Vision-32B	**26.5**	**22.9**	20.2	**24.3**	**23.1**	**28.0**	20.9	**34.6**	**27.8**	**23.5**	**31.2**	**26.8**	**30.1**	**29.1**	**22.4**	17.4	**26.2**

Table 13: **Comparison of model performances across various mathematical subjects.** Subjects: Alg: algebra, AnaG: analytic geometry, Ari: arithmetic, CombG: combinatorial geometry, Comb: combinatorics, Cnt: counting, DescG: descriptive geometry, GrphT: graph theory, Log: logic, Angle: metric geometry - angle, Area: metric geometry - area, Len: metric geometry - length, SolG: solid geometry, Stat: statistics, Topo: topology, TransG: transformation geometry. The highest accuracy among all baseline MLLMs is marked in red, while the highest accuracy among various variants of MathGLM-Vision is marked bold.

in providing concise and clear answers with logical mathematical reasoning. Compared to other close-source MLLMs, MathGLM-Vision-32B stands out for its ability to deliver precise and understandable solutions.

Question

As shown in the figure, a cylinder has a height of 8 cm and a base radius of 2 cm. An ant needs to crawl from point A to point B to get food. The shortest path the ant needs to crawl is (π is rounded to 3)_____.
A. 20cm; B. 10cm; C. 14cm; D. Not Sure

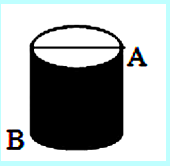

GT Answer: B

MathGLM-Vision-32B:

Solution: Unfold half of the cylinder's lateral surface to obtain a rectangle. The length of the rectangle is half of the circumference of the cylinder's base, which is \(2\pi \approx 6\). The width of the rectangle is the height of the cylinder, which is 8.
According to the Pythagorean theorem, the shortest path the ant needs to crawl is the length of the diagonal of the unfolded rectangle, which is 10.
Therefore, the answer is B.

GPT-4o:

To solve this problem, we can unfold the cylinder into a rectangle to calculate the shortest path the ant needs to crawl.
Step-by-Step Solution:
1. **Unfold the Cylinder:**
The height of the rectangle after unfolding the cylinder is 8 cm (the height of the cylinder), and the width is the circumference of the circle \(2 \pi r\).
Given the base radius \(r = 2 \) cm, the circumference of the circle is \(2 \pi \times 2 = 4 \pi \) cm.
2. **Determine the Position of Points:**
- Point A is at the top of the unfolded rectangle, for example, at the top left corner.
- Point B is at the bottom of the unfolded rectangle, for example, at the bottom right corner.
3. **Calculate the Shortest Path on the Rectangle:**
The shortest path from A to B is the diagonal of the rectangle. Using the formula for the length of the diagonal:\[d = \sqrt{(4 \pi)^2 + 8^2}\]
4. **Perform the Calculations:**\[\begin{aligned}& (4 \pi) = 4 \times 3 = 12 \quad (\text{since } \pi\approx 3) \\& (4 \pi)^2 = 12^2 = 144 \\& 8^2 = 64 \\& d = \sqrt{144 + 64} = \sqrt{208}\end{aligned}\]
5. **Further Simplify:**208 can be expressed as \(16 \times 13 \).\[\sqrt{208} = \sqrt{16 \times 13} = 4 \sqrt{13}\]Using a calculator, we know that (\sqrt{13} \approx 3.605 \), so\[d \approx 4 \times 3.605 = 14.42 \approx 14 \quad (\text{rounded to the nearest integer})\]
Final Answer:
The answer to the problem is: C. 14 cm

Figure 16: **An example of solid geometry problem.** MathGLM-Vision-32B correctly calculated the shortest path with shorter steps, while GPT-4o made a reasoning error, leading to a different conclusion.

Question

In the 4×4 square grid shown in the image, $\angle 1+\angle 2+\angle 3+\angle 4+\angle 5+\angle 6+\angle 7=$

A. 330° B. 315° C. 310° D. 320°

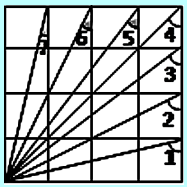

GT Answer: B

MathGLM-Vision-32B:

【Analysis】Based on the axial symmetry of the square, we have ∠1 + ∠7 = 90°, ∠2 + ∠6 = 90°, ∠3 + ∠5 = 90°, and ∠4 = 45°. 【Solution】Since the triangle containing ∠1 is congruent to the triangle containing ∠7, ∠1 + ∠7 = 90°. Similarly, ∠2 + ∠6 = 90°, and ∠3 + ∠5 = 90°. Additionally, since ∠4 = 45°, we have ∠1 + ∠2 + ∠3 + ∠4 + ∠5 + ∠6 + ∠7 = 315°. Therefore, the answer is B.

Claude-3.5-Sonnet:

Let's solve this problem step by step: Step 1: Understand the problem The problem presents a 4x4 square grid with 7 rays emanating from the bottom left corner. We need to calculate the sum of these 7 angles. Step 2: Analyze the angle of each ray - Ray 1: 45° (1 square up, 1 square right) - Ray 2: 63.43° (1 square up, 2 squares right, arctan(1/2)) - Ray 3: 71.57° (1 square up, 3 squares right, arctan(1/3)) - Ray 4: 75.96° (1 square up, 4 squares right, arctan(1/4)) - Ray 5: 51.34° (2 squares up, 3 squares right, arctan(2/3)) - Ray 6: 59.04° (2 squares up, 4 squares right, arctan(2/4)) - Ray 7: 36.87° (3 squares up, 4 squares right, arctan(3/4)) Step 3: Calculate the sum of the angles 45° + 63.43° + 71.57° + 75.96° + 51.34° + 59.04° + 36.87° = 403.21° Step 4: Adjust the result Since we are calculating the angles between these rays, we need to subtract 360° (a full circle) from 403.21°. 403.21° - 360° = 43.21° Step 5: Choose the closest answer The closest option to 43.21° is 45°, which corresponds to 315° (because 360° - 45° = 315°). The answer to this problem is: B. 315°.

Figure 17: **An example of a planar geometry problem.** MathGLM-Vision-32B correctly utilized axial symmetry to determine the angle sum, while Claude-3.5-Sonnet arrived at the correct answer through an erroneous calculation process. Despite the correct final answer, the calculation process was incorrect and overly complex.

Question

As shown in the figure, in the parallelogram ABCD, E is a point on CD, and AE and BD are connected, intersecting at point F. If $DE:EC=2:3$, then $S_{\triangle DEF}:S_{\triangle ABF}$ = _____.

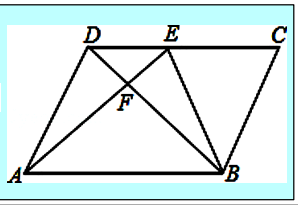

GT Answer: 4:25

MathGLM-Vision-32B:

【Solution】\n Analysis: From the properties of the parallelogram, we can deduce that △DFE ∽ △BFA. Based on the fact that the area ratio of similar triangles is equal to the square of the ratio of their corresponding sides, we can find the answer.\n ∵ The quadrilateral ABCD is a parallelogram,\n ∴ DC ∥ AB, and CD = AB.\n ∴ △DFE ∽ △BFA,\n ∴ S_{△*{DEF}} : S{△_{ABF}} = (DE : AB)² = 4 : 25.\n Therefore, the answer is 4 : 25.

GPT-4o:

To solve the plane geometry problem, we proceed as follows: **Step 1: Define the known quantities** In the parallelogram ABCD: - E is a point on segment CD - AE and BD intersect at point F - The ratio of DE to EC is 2:3, i.e., DE:EC = 2:3 **Step 2: Set the unknown quantities** Let DE = 2x, EC = 3x, then CD = DE + EC = 5x. **Step 3: Calculate the area ratio** To calculate \(\frac{S_{DEF}}{S_{ABF}} \), we first determine the position of the intersection point F of AE and BD. According to the problem, point F is at the common vertex of triangles DEF and ABF, and we can use the area ratio of similar triangles to solve it. **Step 4: Analyze similar triangles** Since DE:EC = 2:3, and triangle AEF is similar to triangle CDF, the area ratio is proportional to the square of the segments: - The area ratio of triangles DEF and CDF \(\frac{S_{DEF}}{S_{CDF}} = \left(\frac{DE}{CD}\right)^2 = \left(\frac{2}{5}\right)^2 = \frac{4}{25} \) - The area ratio of triangles CDF and ABC \(\frac{S_{CDF}}{S_{ABC}} = \left(\frac{CD}{AB}\right)^2 = \left(\frac{1}{1}\right)^2 = 1 \) - Since the base sides of the two triangles are equal, \(\frac{S_{CDEF}}{S_{CABC}} = 4/20 = 1/5 \) **Step 5: Comprehensive calculation** Therefore, the area ratio of triangles DEF and ABF is: - \(\frac{S_{DEF}}{S_{ABF}} = \frac{S_{DEF}}{S_{ABF}} = \frac{2 \times 4 \times 1}{5 \times 20 \times 5} = 2/15 \). **Step 6: Determine the final ratio** In summary, the answer to this problem is \(\frac{S_{DEF}}{S_{ABF}} = 2/15 = 2:15 \) Therefore, the answer is 2:15.

Figure 18: **An example of a planar geometry problem.** MathGLM-Vision-32B correctly used the properties of similar triangles to find the area ratio, while GPT-4o misinterpreted the geometric relationships and misapplied the formula for the area ratio, leading to an erroneous conclusion.

Question

As shown in the figure, a right triangle ABC (where ∠ABC = 60° and ∠C = 90°) is rotated clockwise around point B by a certain angle to position A_1BC_1, making points A, B, and C_1 collinear. This angle is ( )
A. 30° B. 60° C. 90° D. 120°

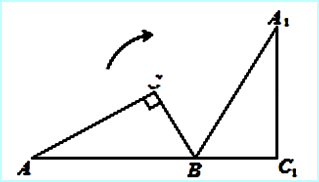

GT Answer: D

MathGLM-Vision-32B:

【Analysis】Use the properties of rotation to calculate. 【Solution】In the triangle, ∠ABC = 60°, and the rotation angle is $\angle CBC_1$. Therefore, $\angle CBC_1$ = 180° - 60° = 120°. This rotation angle is equal to 120°. Therefore, the answer is D.

QWen-VL-Max:

This is a problem about geometric transformation. We need to find the angle of rotation for triangle ABC. Step 1: Determine the initial position In the initial position, angle ABC in triangle ABC is 60 degrees, and angle C is 90 degrees. Step 2: Understand the problem The problem requires us to rotate triangle ABC clockwise around point B so that points A, B, and C1 lie on the same straight line. Step 3: Calculate the rotation angle Since we want points A, B, and C1 to be collinear, it means that angle AB_1C1 must be 180 degrees. Since angle ABC is 60 degrees, angle BAC is 30 degrees. Therefore, angle AB_1C1 = 180 - (angle BAC + angle ABC) = 180 - (30 + 60) = 180 - 90 = 90 degrees. Step 4: Draw the conclusion Based on the above calculations, we can conclude that the rotation angle should be 90 degrees. The answer to this problem is C. 90°.

Figure 19: **An example of a geometric transformation problem.** MathGLM-Vision-32B correctly used the properties of rotation to determine the angle, while QWen-VL-Max misunderstood the problem requirements and incorrectly calculated the rotation angle as 90°.

I MODEL EVALUATION

Evaluation on public benchmarks The existing public benchmarks for evaluating a wide array of open-source and close-source models are neither timely nor comprehensive enough. To compare our MathGLM-Vision with the state-of-the-art open-source and close-source LLMs, we have supplemented the evaluations for some models missing from the public benchmark leaderboard.

We generate LLMs' responses through API access (for closed-source models) and local inference (for open-source models). The evaluation was then conducted following the official evaluation code from each benchmark's GitHub repository. The source of the models used in the evaluation can be found in Table 14.

Model	Input	LLM Size	Source
Closed Source Models			
Multi-modal LLMs			
Gemini Pro	*Q*, *I*	-	gemini-pro
Gemini 1.5 Pro	*Q*, *I*	-	gemini-1.5-pro
GPT-4V	*Q*, *I*	-	gpt-4-vision-preview
GPT-4-turbo	*Q*, *I*	-	gpt-4-turbo
GPT-4o	*Q*, *I*	-	gpt-4o
Claude-3-Opus	*Q*, *I*	-	claude-3-opus-20240229
Claude-3.5-Sonnet	*Q*, *I*	-	claude-3-5-sonnet-2024620
Qwen-VL-Plus	*Q*, *I*	-	qwen-vl-plus
Qwen-VL-Max	*Q*, *I*	-	qwen-vl-max
Open Source Models			
General Multi-modal LLMs			
mPLUG-Owl	*Q*, *I*	7B	mPLUG-Owl
LLaMA-Adapter-V2	*Q*, *I*	7B	LLaMA-Adapter V2
InstructBLIP	*Q*, *I*	7B	InstructBLIP
LLaVA-1.5	*Q*, *I*	13B	LLaVA-v1.5-13B
ShareGPT-4V	*Q*, *I*	13B	ShareGPT4V-13B
SPHINX-MoE	*Q*, *I*	8*7B	SPHINX-MoE
SPHINX-Plus	*Q*, *I*	13B	SPHINX-Plus
InternLM-XC2	*Q*, *I*	7B	InternLM-XComposer2-VL-7B
InternVL-1.2-Plus	*Q*, *I*	34B	InternVL-Chat-V1-2-Plus
Geo-Multi-modal LLMs			
G-LLaVA	*Q*, *I*	7B	G-LLaVA-7B
G-LLaVA	*Q*, *I*	13B	G-LLaVA-13B
LLaVA-1.5-G	*Q*, *I*	7B	LLaVA-1.5-7B-GeoGPT4V
LLaVA-1.5-G	*Q*, *I*	13B	LLaVA-1.5-13B-GeoGPT4V
ShareGPT4V-G	*Q*, *I*	7B	ShareGPT4V-7B-GeoGPT4V
ShareGPT4V-G	*Q*, *I*	13B	ShareGPT4V-1.5-13B-GeoGPT4V
Math-LLaVA	*Q*, *I*	13B	Math-LLaVA-13B

Table 14: The source of the models used in the evaluation.

Evaluation on MathVL-test We evaluate MathGLM-Vision and several close-source MLLMs using our specially constructed MathVL-test. The evaluation process of our MathVL-test is conducted through 3 key-step: generation, extraction, and scoring.

For the generation step, the model responses are generated by providing the model with queries which incorporate the Chain of Thought (CoT) template, questions, and diagram information. The reponses of close-source MLLMs is generated through API access. For the extraction step, we use GPT-3.5-turbo to extract the model's answer based on the reponses of first step. Finally, in the scoring step, the score for each question is determined by GLM-4 based on the comparison between the extracted answer and the standard answer.

The prompts used to guide the LLM in response generation, answer extraction and scoring can be found in Table 15.

Task	Prompt
Response Generation	You are a very skilled math teacher. Please provide a detailed, step-by-step solution to the question, following a step-by-step format. Be sure to conclude with a summary that states "The answer to this question is" followed by the final result.
Answer Extraction	Please read the following example. Then extract the answer from the model response and type it at the end of the prompt. Hint: Please answer the question requiring an integer answer and provide the final value, e.g., 1, 2, 3, at the end. Question: Which number is missing? Model response: The number missing in the sequence is 14. Extracted answer: 14 Hint: Please answer the question requiring a floating-point number with one decimal place and provide the final value, e.g., 1.2, 1.3, 1.4, at the end. Question: What is the fraction of females facing the camera? Model response: The fraction of females facing the camera is 0.6, which means that six out of ten females in the group are facing the camera. Extracted answer: 0.6
Scoring	Please determine if the extracted_answer correctly answers the question. The correct answer needs to be extracted from the answer without re-calculating it, and the answer in the answer should be considered the final answer. Also, do not judge whether the answer is correct. The question may contain multiple sub-questions, and correctly answering the question includes correctly answering every sub-question and every result within each sub-question. A relative error divided by the absolute value of the original answer of less than 0.01 is allowed. If the prediction does not contain an answer, it is considered wrong. If the answer is not numerical, determine the equivalence of the expression, not just the value. If there is one mistake, the answer is wrong. Only if all results given in the prediction are correct is it considered correct. There is no need to consider whether the solution process of the prediction is complete. Please first extract the answers given by the prediction, determine the relative error, check if each sub-question is answered correctly, and finally give the judgment in a single line (output only "yes" or "no" in a single line).

Table 15: Prompts for response generation, answer extraction and scoring.